Healthspan improvement and anti-aggregation effects induced by a marine-derived structural proteasome activator

Mary A. Vasilopoulou [a,b], Anna Gioran [a], Margarita Theodoropoulou [a], Aikaterini Koutsaviti [c], Vassilios Roussis [c], Efstathia Ioannou [c], Niki Chondrogianni [a,*]

[a] *Institute of Chemical Biology, National Hellenic Research Foundation, 48 Vassileos Constantinou Ave., Athens, 11635, Greece*
[b] *Department of Biochemistry and Biotechnology, University of Thessaly, Biopolis, 41500, Larissa, Greece*
[c] *Section of Pharmacognosy and Chemistry of Natural Products, Department of Pharmacy, School of Health Sciences, National and Kapodistrian University of Athens, Panepistimiopolis Zografou, Athens, 15771, Greece*

ARTICLE INFO

ABSTRACT

Proteasome activation has been shown to promote cellular and organismal healthspan and to protect against aggregation-related conditions, such as Alzheimer's disease (AD). Various natural compounds have been described for their proteasome activating properties but scarce data exist on marine metabolites that often possess unique chemical structures, exhibiting pronounced bioactivities with novel mechanisms of action. In this study, we have identified for the first time a marine structural proteasome activator, namely (1*R*,3*E*,6*R*,7*Z*,11*S*,12*S*)-dolabella-3,7,18-trien-6,17-olide (DBTO). DBTO activates the 20S proteasome complex in cell-free assays but also *in cellulo*. Continuous supplementation of human primary fibroblasts with DBTO throughout their cellular lifespan confers an improved healthspan while ameliorated health status is also observed in wild type (wt) *Caenorhabditis elegans* (*C. elegans*) nematodes supplemented with DBTO. Furthermore, treatment of various AD nematode models, as well as of human cells of neuronal origin challenged with exogenously added Aβ peptide, with DBTO results in enhanced protection against Aβ-induced proteotoxicity. In total, our results reveal the first structural proteasome activator derived from the marine ecosystem and highlight its potential as a compound that might be used for healthspan maintenance and preventive strategies against proteinopathies, such as AD.

1. Introduction

Aging is a physiological, unavoidable process characterized by gradual dyshomeostasis, accompanied by accumulation of damage in all vital cellular building blocks that eventually leads to death. Both genetic and environmental factors regulate its progression [1]. Aging also represents a major risk factor for the development of neurodegenerative diseases, including Alzheimer's disease (AD) [2]. AD is the most common form of dementia characterized by gradual loss of cognitive function that affects a large proportion of the aged population [3]. The accumulation and aggregation of the extracellular amyloid-β (Aβ) peptide in plaques is one of its main neuropathological features. One of the priorities in the anti-aging field is the identification of naturally occurring bioactive compounds that may affect/alter specific molecular pathways that are deregulated during aging or upon age-related

diseases. Ideally, these natural products would improve human health with minimal side effects.

The proteasome is a multi-catalytic enzymatic complex with a pivotal role in the maintenance of protein homeostasis (proteostasis). It is implicated in the regulated proteolysis of normal and abnormal in any way proteins, as well as of partially or loosely unfolded proteins [4]. Proteasomes consist of the core particle, also known as the 20S proteasome, while its capping with either one or two regulatory particles gives rise to the 26S or 30S proteasomes, respectively [5]. Although the 20S proteasome was believed to exclusively participate in the ubiquitin-independent proteolysis [6], it was recently shown that the 20S proteasome can also degrade the ubiquitin tag along with the conjugated substrate, albeit with different rates [7]. Moreover, it was shown that enhanced 20S proteasome levels are responsible for cell survival against stress associated with damaged proteins [7]. Seven different α and β subunits compose the 700 kDa barrel-shaped 20S core arranged in

---

Abbreviations

Alzheimer's disease	AD
amyloid-β	Aβ
amyloid precursor protein	APP
Caenorhabditis elegans	*C. elegans*
caspase-like	C-L
chymotrypsin-like	CT-L
Conditioned medium from CHO cell line	CM
conditioned medium from CHO-7PA2 cell line	CM$_{Aβ}$
Cumulative Population Doublings	CPD
geneticin	G418
green fluorescent protein	GFP
2′,7′-dichlorodihydrofluorescein diacetate	H2DCFDA
Heme Oxygenase 1	HO-1
Huntington's disease	HD
methyl coumarin	MCA
NAD(P)H quinone oxidoreductase-1	NQO-1
nitroblue tetrazolium chloride	NBT
nuclear factor (erythroid-derived-2)-like 2	Nrf2
phenazine methosulfate	PMS
population doublings	PD
Reactive Oxygen Species	ROS
senescence-associated-β-galactosidase	SA-β-gal
sodium dodecyl sulfate	SDS
Superoxide dismutase	SOD
trypsin-like	T-L
wild type	wt
(1*R*,3*E*,6*R*,7*Z*,11*S*,12*S*)-dolabella-3,7,18-trien-6,17-olide	DBTO
18α-glycyrrhetinic acid	18α-GA

---

a $\alpha_{1-7}\beta_{1-7}\beta_{1-7}\alpha_{1-7}$ configuration. Three β subunits, namely β1, β2, and β5 represent the catalytic subunits responsible for the caspase-like (C-L; β1 subunit), trypsin-like (T-L; β2 subunit) and chymotrypsin-like (CT-L; β5 subunit) activities [5].

The proteasome in its various forms represents one of the main cellular secondary antioxidant mechanisms that is under tight redox control [8]. Thus, it is not surprising that an age-related impairment of the proteasome function in both *in vitro* and *in vivo* aging models (where redox status is altered) has been revealed. As aging progresses, the proteasome content and function diminish [9]. In contrast, cultured fibroblasts from healthy centenarians maintained their proteasomes active compared to cultures from old donors [10], thus potentially indicating the importance of preserved functional proteasomes for a successful aging process. Indeed, enhanced proteasome levels and/or function accomplished either genetically through the overexpression of 20S [11–14] and 19S [15] proteasome subunits or through natural compounds [16–18] resulted in cellular and organismal lifespan extension and healthspan improvement. The latter has attracted increasing interest over the last few years since the importance of maintaining the well-being for longer, thus reducing frailty, even in the absence of lifespan extension, has been widely recognized [19].

There is also emerging evidence that the proteasome plays a crucial role in AD onset and progression. More specifically, impaired proteasome activities have been found in post-mortem samples of AD patients [20] and in brain samples of transgenic AD mice [21,22]. Moreover, decreased expression levels of 20S proteasome subunits have been observed in both *in vitro* and *in vivo* AD models. Conversely, proteasome activation achieved through the overexpression of the 20S proteasome subunit *pbs-5* (homolog of β5 in *C. elegans*) delayed paralysis onset and progression in an AD and a Huntington's disease (HD) nematode model [11], while the overexpression of the *rpn-6* 19S proteasome subunit has been shown to delay HD-related paralysis in the respective HD nematode model [15]. More recently, ameliorated AD-like pathology in mouse and fly models overexpressing the amyloid precursor protein (APP) through enhanced proteasome activity has also been suggested [23]. Likewise, proteasome activation through a triterpene, namely 18α-glycyrrhetinic acid (18α-GA), conferred resistance to Aβ-induced proteotoxicity in various AD nematode models, as well as to murine cortical neurons exogenously supplemented with enhanced concentrations of Aβ peptide [17]. Similar positive results have also been observed for other natural compounds in various AD models [24,25].

It is worth noting that the majority of the natural products that have been described for their anti-aggregation properties and neuroprotective effects on AD models are of terrestrial origin, while only few are derived from marine organisms [26]. Marine metabolites, quite less explored as compared to compounds of terrestrial origin, often feature diversified chemical structures with novel carbocycles or uncommon functional groups, displaying more potent biological activities. Despite the above, only one study has directly linked the marine-derived polysaccharide fucoidan to elevated proteasome function and subsequent protection against Aβ-induced toxicity in an AD nematode model [27]. Nevertheless, the fucoidan studied was not chemically characterized and the mode of proteasome activation (direct or indirect effect on proteasome structure and activity) was not revealed in that study. Herein, we identify for the first time a natural product isolated from the brown alga *Dictyota mediterranea* collected in the Aegean Sea, namely (1*R*,3*E*,6*R*,7*Z*,11*S*,12*S*)-dolabella-3,7,18-trien-6,17-olide (DBTO, **1**) that acts as a proteasome activator in cell-free assays thus potentially through direct stereochemical interaction with the 20S core, termed as structural activator hereafter (Fig. 1). We have investigated the potential beneficial effects of DBTO on AD onset and progression by taking advantage of AD nematode models and human cells of neuronal origin. In addition, we provide evidence on the role of this compound as a facilitator of healthspan.
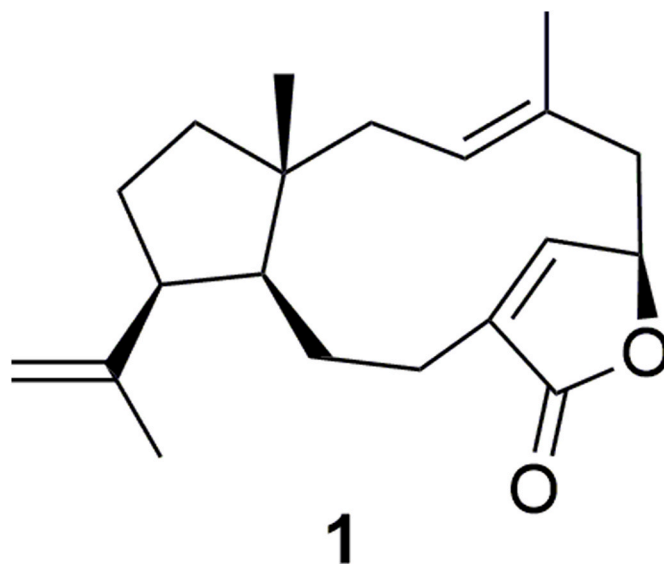

Fig. 1. Chemical structure of compound 1. Chemical structure of (1*R*,3*E*,6*R*,7*Z*,11*S*,12*S*)-dolabella-3,7,18-trien-6,17-olide (DBTO, compound **1**).

2. Materials and methods

2.1. General experimental procedures for isolation and structure elucidation

Normal- and reversed-phase column chromatography separations were performed with Kieselgel Si 60 (Merck, Darmstadt, Germany) and Kieselgel RP-18 (Merck, Darmstadt, Germany), respectively. Normal phase HPLC separations were conducted using an Agilent 1100 liquid chromatography system equipped with refractive index detector (Agilent Technologies, Waldbronn, Germany) or a Cecil 1100 Series liquid chromatography pump (Cecil Instruments Ltd., Cambridge, UK) equipped with a GBC LC-1240 refractive index detector (GBC Scientific Equipment, Braeside, VIC, Australia), using an Econosphere Silica 10u (250 × 10 mm, Grace, Columbia, MD, USA), Kromasil 100-10-SIL (250 × 10 mm, Akzonobel, Eka Chemicals AB, Separation Products, Bohus, Sweden), or Supelcosil SPLC-Si 5 μm (250 × 10 mm, Supelco, Bellefonte, PA, USA) column. Reversed phase HPLC was conducted on an Agilent 1100 liquid chromatography system equipped with refractive index detector (Agilent Technologies, Waldbronn, Germany), using a Kromasil 100C18 (25 cm × 8 mm i.d.) column (MZ-Analysentechnik GmbH, Mainz, Germany). Chiral HPLC separations were conducted on a Pharmacia LKB 2248 liquid chromatography pump (Pharmacia LKB Biotechnology, Uppsala, Sweden) equipped with an RI-102 Shodex refractive index detector (ECOM spol. s r.o., Prague, Czech Republic), using a Chiralcel OD, 10 μm (25 cm × 10 mm, Daicel Chemical Industries Ltd., Osaka, Japan) column. TLC was performed with Kieselgel 60 F254 aluminum-backed plates (Merck, Darmstadt, Germany) and spots were visualized after spraying with 15% (v/v) H_2SO_4 in MeOH reagent and heating at 100 °C for 1 min. The 1D and 2D NMR spectra were recorded on Bruker AC 200, DRX 400, Avance III 600 and Avance NEO 700 (Bruker BioSpin GmbH, Rheinstetten, Germany) spectrometers, using standard Bruker pulse sequences at room temperature. Chemical shifts are given on a δ (ppm) scale using TMS as the internal standard. High-resolution ESI or APCI mass spectra were measured on a Thermo Scientific LTQ Orbitrap Velos mass spectrometer (Thermo Fisher Scientific, Bremen, Germany). Low-resolution EI mass spectra were measured on a Hewlett-Packard 5973 mass spectrometer (Agilent Technologies, Santa Clara, CA, USA). Low-resolution CI mass spectra were measured on a Thermo Electron Corporation DSQ mass spectrometer (Thermo Electron Corporation, Austin, TX, USA) using a direct-exposure probe with CH_4 as the reagent gas. IR spectra were obtained on a Bruker Alpha II (Bruker Optik GmbH, Ettlingen, Germany) spectrometer. UV spectra were obtained on a Shimadzu UV-1900i (Shimadzu Europa GmbH, Duisburg, Germany) spectrophotometer. Optical rotations were measured on a Krüss model P3000 polarimeter (A. KRÜSS Optronic GmbH, Hamburg, Germany) with a 0.5 dm cell.

2.2. Isolation and structure elucidation of DBTO

Specimens of *Dictyota mediterranea* were collected from Agios Theodoros bay at the island of Karpathos in August of 2013. The alga was washed with seawater to remove epiphytes and debris, rinsed thoroughly with fresh water, immediately frozen and transferred to the laboratory, where it was kept at −20 °C until further processed. The fresh frozen algal biomass was thoroughly extracted with mixtures of CH_2Cl_2/MeOH at room temperature. After evaporation of the solvents *in vacuo*, the organic extract (8.46 g) was subjected to vacuum liquid chromatography on silica gel, using cHex with increasing amounts of EtOAc, followed by EtOAc with increasing amounts of MeOH as mobile phase, to afford seven fractions (DMK1–DMK7). Fraction DMK2 (10–15% EtOAc in cHex, 676.0 mg) was further subjected to gravity column chromatography on silica gel, using mixtures of cHex with increasing amounts EtOAc as the mobile phase, to yield 12 fractions (DMK2a–DMK2l). DMK2k (10% EtOAc in cHex, 26.5 mg) was purified by normal phase HPLC, using cHex/EtOAc (93:7) as eluent, to afford

compound **1** (2.7 mg). Fraction DMK3 (20–25% EtOAc in cHex, 747.0 mg) was subjected to vacuum liquid chromatography on silica gel, using CH_2Cl_2 with increasing amounts of EtOAc as the mobile phase, to yield eight fractions (DMK3a–DMK3h). Fraction DMK3a (100% CH_2Cl_2, 28.5 mg) was purified by normal phase HPLC, using cHex/EtOAc (93:7) as eluent, to afford compound **1** (23.2 mg). Compound **1** was identified, after thorough analysis of its NMR and MS spectroscopic data and comparison of its spectroscopic and physical characteristics with those reported in the literature, as (1*R*,3*E*,6*R*,7*Z*,11*S*,12*S*)-dolabella-3,7,18-trien-6,17-olide, previously isolated from the extract of *Trichilia trifolia* [28]. Compound **1**, as well as the remaining metabolites evaluated during the initial screening (Fig. S1), were stored at −20 °C until analyzed.

2.3. Reagents and antibodies

The following primary antibodies were used: β1 (BML-PW8140; Enzo Life Sciences, Lausen, Switzerland), β2 (PW8145; Enzo Life Sciences, Lausen, Switzerland), β5 (PW8895; Enzo Life Sciences, Lausen, Switzerland), α6 (PW8100; Enzo Life Sciences, Lausen, Switzerland), α7 (PW8110; Enzo Life Sciences, Lausen, Switzerland), p21 Waf1/Cip1 (12D1) (2947; Cell Signaling, Danvers, MA, USA), 6E10 (803001; BioLegend, San Diego, USA), Rb x Amyloid oligomer (AB9234; Millipore, Burlington, MA, USA), heme Oxygenase-1 (HO-1) (sc-10787, Santa Cruz Biotechnology, Heidelberg, Germany), NAD(P)H quinone oxidoreductase-1 (NQO1) (C19) (sc-16484, Santa Cruz Biotechnology, Heidelberg, Germany), GAPDH (sc-47724; Santa Cruz Biotechnology, Heidelberg, Germany), actin (691002; MP Biomedicals, Santa Ana, USA). Secondary antibodies were purchased from Santa Cruz Biotechnology (Heidelberg, Germany).

2.4. Cell lines and culture conditions

HFL1 human embryonic primary fibroblasts (ECACC 89071902) were obtained from the European Collection of Cell Cultures and maintained in Dulbecco's modified Eagle's medium (DMEM; Invitrogen, Carlsbad, CA, USA) supplemented with 10% fetal bovine serum (Invitrogen, Carlsbad, CA, USA), 2 mM glutamine, 1% non-essential amino acids and 1% penicillin-streptomycin (complete medium).

The human neuroblastoma cell line SH-SY5Y was maintained in DMEM supplemented with 10% fetal bovine serum and 1% penicillin-streptomycin. SH-SY5Y cells were treated with conditioned medium produced by (a) the control cell line Chinese hamster ovary (CHO); CM and, (b) the Aβ-producing cell line 7PA2, derived following stable transfection of CHO cells with human APP751 bearing the Val717Phe familial AD mutation that leads to Aβ overproduction [29]; $CM_{Aβ}$ (conditioned media containing Aβ peptide). Both CHO and CHO-7PA2 cell lines were maintained in RPMI 1640 medium supplemented with 10% fetal bovine serum, 2 mM glutamine, and 1% penicillin-streptomycin with 150 μg/mL geneticin (G418; ThermoFisher Scientific, Bremen, Germany) (complete RPMI medium).

To produce conditioned media (CM/$CM_{Aβ}$), CHO and 7PA2 cells were grown to ∼ 90% confluency, washed with phosphate-buffered saline (PBS; Invitrogen, Carlsbad, CA, USA) and incubated in serum-free complete RPMI medium (without G418) for ∼ 16 h. The CM/$CM_{Aβ}$ was collected and centrifuged to remove cell debris. SH-SY5Y cells were pre-treated with 0.3 μg/mL DBTO or DMSO and 20 nM epoxomicin (UBPBio, Aurora, USA) wherever indicated for 24 h and were then exposed to the relative conditioned medium derived from CHO cells (CM) or 7PA2 cells ($CM_{Aβ}$) supplemented with 0.3 μg/mL DBTO or DMSO and 20 nM epoxomicin wherever indicated. Cells were sub-cultured at 37 °C, 5% CO_2 and 95% humidity.

Cell viability assay: Cell viability of SH-SY5Y cultures was assessed through scoring of attached CM/$CM_{Aβ}$-treated SH-SY5Y cells after 24 h of incubation in triplicates using a Coulter Z_2 counter.

Survival ratio through crystal violet staining: SH-SY5Y cells treated as

described above were fixed in 4% paraformaldehyde for 20 min and then stained with 0.2% crystal violet in distilled water. Cells were washed with water, air-dried and the dye was eluted with 30% acetic acid. Viability was assessed through measurement of dye absorbance at 595 nm using the Safire^2 Multi-detection Microplate Reader (Tecan, Grodig, Austria).

2.5. Cell and nematode treatment with DBTO

Cell treatment: HFL1 human primary fibroblasts and SH-SY5Y human dopaminergic neuroblastoma cells were treated with 0.3 μg/mL (0.998 μM) DBTO for 2 h or 24 h unless otherwise indicated.

Nematode treatment: Nematodes were exposed to 5 μg/mL (16.642 μM) final concentration of DBTO per NGM plate. Stock solutions of DBTO were prepared after suspension in DMSO and were kept at −20 °C. The appropriate amount of DBTO or DMSO (<0.1%; control) [30,31] was added on the UV-irradiated OP50 bacteria lawn. UV-killed bacteria were used to avoid the side effects of living bacteria metabolism.

Continuous cell treatment for lifespan experiments: Early passage (cumulative population doublings (CPD) < 32) HFL1 cells (55×10^3) were treated continuously throughout their lifespan with 0.3 or 0.5 (1.664 μM) or 5 μg/mL DBTO until they entered senescence. Control cultures were supplemented with 0.1% DMSO. The compound (DBTO or DMSO) was renewed every other day. Upon 90% confluence, cell number was determined in triplicates using a Coulter Z2 counter and the population doublings (PD) were calculated using the formula: log (Nf/N0)/log 2, where Nf is the number of cells measured when each culture reached confluence and N0 represents the number of cells initially seeded.

2.6. Proteasome activity assay

Early passage HFL1 cells (CPD) < 32) were seeded in petri dishes (5 $\times 10^5$ cells) and were treated with 0.3 μg/mL DBTO or the diluent (0.1% v/v DMSO) for 2 h the following day. SH-SY5Y cells (65×10^4) were seeded in petri dishes and 24 h later, they were treated with 0.3 μg/mL DBTO or the diluent (0.1% v/v DMSO) for 24 h. Cells were collected in lysis buffer (20 mM Tris-HCl pH 7.6, 1 mM EDTA, 20 mM KCl, 10% glycerol, 0.2% Nonidet P-40, 5 mM ATP, 1 mM dithiothreitol, 10 mg/mL aprotinin, and 10 mM phenylmethylsulfonyl fluoride) and were incubated at 4 °C for 30 min. Lysates were centrifuged at 13.000 rpm for 10 min and the supernatants were used to determine the proteasome activities, following incubation of 10 μg of total protein in the presence of the Suc-LLVY-AMC, Boc-LRR-AMC, Z-LLE-AMC fluorogenic peptides for the determination of CT-L, T-L and C-L proteasome activities, respectively (UBPBio, Aurora, USA). To test the potential properties of DBTO as a structural activator, 0.5 μg of highly purified human 20S proteasome (Protein Center Kibbuzt Ramat Yohana, Haifa, Israel) was incubated with various concentrations of the examined compound or 0.01% w/v sodium dodecyl sulfate (SDS; positive control) or 20 μM MG132 (negative control) in the presence of the above-mentioned specific fluorogenic peptides (UBPBio, Aurora, USA). In all cases, methyl coumarin (MCA) liberation was measured every 5 min using the Safire^2 Multi-detection Microplate Reader (Tecan, Grodig, Austria) at $\lambda_{ex} = 380$ nm, $\lambda_{em} = 460$ nm at 37 °C for 30 min. Proteasome activity was determined as a percentage (%) of the relative specific proteasome activity in control-treated cells or the relative sample (in the case of the purified 20S proteasome) that was set to 100%. Protein concentrations were determined using the Bradford method with bovine serum albumin (BSA) as standard.

2.7. Senescence associated-β-galactosidase staining

Staining for senescence-associated-β-galactosidase (SA-β-gal) activity was performed as previously described [32]. Briefly, 10^5 cells were seeded in 6-well plates. After 24 h cells were washed with PBS, fixed with 0.2% glutaraldehyde and 2% formaldehyde for 5 min, washed

again with PBS and stained at 37 °C in the absence of CO_2 in staining solution (150 mM NaCl, 2 mM $MgCl_2$, 5 mM $K_3Fe(CN)_6$, 40 mM citric acid, 12 mM sodium phosphate, pH 6.0) containing 1 mg/mL of 5-bromo-4-chloro-3-indolyl-β-D-galactosidase (Duchefa Biochemie, Haarlem, Netherlands). The results are expressed as the ratio of SA-β-gal positive cells to the total number of cells in each sample.

2.8. Scratch assay

The migration and proliferation of cells treated with 0.3 μg/mL DBTO or DMSO (control) were assessed using the *in vitro* scratch assay, as previously described [33]. Briefly, cells treated with 0.3 μg/mL DBTO or DMSO throughout their lifespan (starting from an early passage, CPD<32) were seeded in 6-well plates at different lifespan time points (following 28 and 60 days of continuous treatment either with DBTO or DMSO). When they reached confluence, the culture was scratched to form a "technical wound" (gap) across the plate using a P200 pipette tip. The debris was removed through washing with the culture medium and then fresh medium containing 0.3 μg/mL DBTO or DMSO was added. Cell cultures were monitored until closure of the gaps. Pictures were taken 24 and 48 h after the gap formation. In the case of very early passage cells (CPD<40), only the first time point (24 h) was evaluated since the cultures then became confluent.

2.9. Nematode strains and growth conditions

Standard procedures were followed for *C. elegans* cultures growth and maintenance. All strains were kept at 20 °C except for CL4176 and CL2331 that were maintained at 16 °C. The following strains were used: N2 [wt Bristol isolate; wt], CL4176: *dvIs27 [pAF29(myo-3p:A-Beta (1–42)::let-851 3′UTR) + (pRF4(rol-6(su1006))]*, CL2331: *dvIs37 [myo-3p::GFP::A-Beta (3–42) + rol-6(su1006)]*.

2.10. Paralysis assay

Synchronized CL4176 animals (300–600 animals per condition) were transferred to NGM plates containing either 5 μg/mL DBTO or DMSO at 16 °C for 48 h before temperature upshift to 25 °C. Scoring of paralyzed animals was initiated 24 h after the temperature upshift. The paralysis assay was repeated six times. Nematodes were scored as paralyzed if they exhibited halos of cleared bacteria around their heads or failed to undergo half-end body wave propagation upon prodding. Animals that died were excluded. The log-rank (Mantel-Cox) test was used to evaluate differences between paralysis curves and to determine p values for all independent data. N in paralysis figures is the number of paralyzed animals over the total number of animals used (the number of paralyzed animals plus the number of animals that died and the number of censored animals due to internally hatched eggs, protruding vulva or desiccation due to crawling off the plates). Median paralysis values are expressed as mean ± SEM.

2.11. Confocal analysis of Aβ deposition

For $A\beta_{3-42}$ deposit measurements, synchronized CL2331 animals were exposed to 5 μg/mL DBTO or DMSO and grown at 20 °C (to induce the expression of the $A\beta_{3-42}$ peptide) until day 1 of adulthood. Animals were mounted on 2% agarose pads on glass slides, anesthetized with 100 mM levamisole and observed at room temperature using a Leica TSC SPE confocal laser scanning microscope (Leica Lasertechnik GmbH, Heidelberg, Germany). The LAS AF software was used for image acquisition. Images focused in the anterior area of the nematodes were acquired with a 20/0.70 objective. The number of aggregates was counted in at least 25 animals/condition.

2.12. Phenotypic analysis

For all assays, N2 animals were allowed to lay eggs for 20–30 min on NGM plates containing either 5 μg/mL DBTO or DMSO. The following phenotypic characteristics were monitored:

Pharyngeal pumping: At day 1 of adulthood, the pharyngeal pumping rate was measured. 50 animals per condition were examined.

Defecation assay: At day 1 of adulthood, the defecation rate (period in seconds from defecation to defecation) was measured. 50 animals per condition were examined.

Developmental timing: The progeny was frequently observed to record the needed time to reach the L4 larval stage from egg hatching. The experiment was repeated three times.

Fecundity assay: Single N2 L4 larvae were transferred on NGM plates containing either 5 μg/mL DBTO or DMSO. Each animal was transferred every two days to a fresh NGM plate containing 5 μg/mL DBTO or DMSO. Progeny of each animal was scored at the L2-L3 larval stage. At least 10 animals per condition were examined.

Dauer formation: The progeny was kept at 27 °C and the number of animals at the dauer larval stage over the total number of animals was scored 72 h later. The experiment was repeated three times.

2.13. Immunoblot and dot blot analysis

20 μg of proteins extracted in the lysis buffer described in section 2.6 were separated by 12% SDS-PAGE according to standard procedures [34]. Proteins were then transferred to nitrocellulose membranes for probing with appropriate antibodies. For dot blot analysis, when 50% of the control population got paralyzed, all alive animals were collected and boiled in non-reducing Laemmli buffer. Subsequently, 5 μg of protein lysates were spotted onto 0.2 μm nitrocellulose membranes. Immunoblotting was performed using the 6E10 antibody (BioLegend, San Diego, USA) that recognizes total Aβ species and Rb x Amyloid oligomer antibody (Millipore, Burlington, MA, USA) that recognizes all types of Aβ oligomers. Secondary antibodies conjugated with horseradish peroxidase and enhanced chemiluminescence were used to detect the bound primary antibodies. All blots were developed with chemiluminescence using the Clarity™ Western ECL substrate (Bio-Rad Laboratories, Hercules, USA) in a ChemiDoc station (Bio-Rad Laboratories, Hercules, USA). Actin (for nematodes) or GAPDH (for cells) were used as a loading control. Densitometry analysis for the quantification of blots was performed with Bio-Rad's Image Lab software 6.0.1 or ImageJ 1.52a (Bio-Rad Laboratories, Hercules, USA). Quantification of the ratio of each protein to actin or GAPDH and normalization to control appear next to each representative blot. Each immunoblot analysis was performed three times unless otherwise indicated and representative blots are shown. The molecular weight of each protein appears on the right of each blot.

2.14. Determination of reactive oxygen species (ROS)

2′,7′-dichlorodihydrofluorescein diacetate (H2DCFDA, Molecular Probes, Invitrogen Ltd, Carlsbad, CA, USA) was used for ROS detection. Early passage HFL1 cells (CDP <32) were seeded in petri dishes (5×10^5 cells) and were treated with 0.3 μg/mL DBTO or the diluent (0.1% v/v DMSO) for 2 h the following day. The cell number in each sample was determined and 10^5 cells were resuspended in pre-warmed PBS in the presence or absence (control sample) of the dye at a final concentration of 10 μM (loading buffer) and incubated at 37 °C for 30 min. Cells were then centrifuged, resuspended in complete medium and incubated at 37 °C for 5 min. The absorption and the emission of the oxidation product were measured at 493 and 520 nm respectively. Each sample was measured in quadruplicates. The experiment was repeated three times.

2.15. Determination of superoxide dismutase (SOD) activity

Cell pellets were collected and lysed via sonication in RIPA buffer supplemented with proteinase inhibitors. Lysates were centrifuged and the supernatant was collected. Protein concentration in the supernatant was determined with DC assay (Bio-Rad Laboratories, Hercules, USA). The protein concentration was adjusted at 0.4 μg/μL for each sample. 25 μL of each lysate (10 μg) were mixed with either 107.5 μL 16 mM Tris-HCl, pH 8.0, 12.5 μL 300 μM nitroblue tetrazolium chloride (NBT), 12.5 μL 468 μM NADH and 12.5 μL 60 μM phenazine methosulfate (PMS) (Sample) or the same combination without PMS (Sample') and loaded in a transparent 96 well plate. Two wells were also prepared with all components but instead of protein, 25 μL of RIPA buffer were loaded (Blank). The plate was incubated in the dark for 10 min and the absorbance was measured with the Safire^2 Multi-detection Microplate Reader (Tecan, Grodig, Austria) at 560 nm. To calculate the SOD activity, the following formula was used: [(A0-A1)/A0]*100, where A0 is the absorbance of the Blank and A1 the absorbance of the Sample when the absorbance of Sample' has been subtracted.

2.16. Statistical analysis

Statistical analysis and graphs were produced using GraphPad Prism 6 (GraphPad Software, Inc.) and Microsoft Office 365 Excel (Microsoft Corporation) software packages. Data in all assays (including blot quantification) are depicted as the average of three independent experiments (unless otherwise indicated). Error bars denote ±SEM. Ordinary one-way ANOVA with Dunnett's post hoc correction was used for multiple comparisons of means. Unpaired *t*-test was used for comparisons of two groups. Asterisks denote p values as follows: *p < 0.05, **p < 0.01, ***p < 0.001, ****p < 0.0001, ns; not significant.

3. Results

3.1. DBTO activates the 20S proteasome in vitro in cell-free assays

Due to the low number of studies reporting the effects of marine natural products on the proteasome [26], we initially screened a panel of structurally diverse compounds isolated from marine macro- and micro-organisms for their potential to act as structural proteasome activators, thus activating the proteasome in cell-free lysates through direct stereochemical alterations. We selected and tested 24 metabolites belonging to different chemical classes, including sesquiterpenes, diterpenes, triterpenes, steroids, carotenoids, acetogenins, nitrogenous compounds and sulfur-containing compounds, obtained from marine organisms of the eastern Mediterranean Sea (Fig. S1). More specifically, we incubated highly purified human 20S proteasome with various concentrations of the selected compounds to evaluate their potential stimulating properties on CT-L proteasome activity in the test tube, in the absence of cell lysates [35,36] (Fig. 2). Based on this initial screening, we identified a dolabellane diterpene (metabolite **xi**; Fig. 2), namely (1*R*,3*E*, 6*R*,7*Z*,11*S*,12*S*)-dolabella-3,7,18-trien-6,17-olide (DBTO, **1**), that enhanced CT-L activity by 1.9- and 3.2-fold following incubation of the 20S proteasome with 20 μg/mL (66.5 μM) or 30 μg/mL (99.8 μM), respectively (Fig. 3a, i). SDS, which favors the opening of the α-gated channel, was used as a positive control [37]. Similar results were obtained for both C-L (Fig. 3a, ii) and T-L proteasome activities (Fig. 3a, iii) in the presence of DBTO. To assure the specificity of the assay, the proteasome inhibitor MG132 was also used. Taken together, these data indicate that DBTO enhances all three proteasome activities in the test tube in cell-free assays and suggest that it may act as a structural 20S proteasome activator through direct stereochemical interaction with the 20S complex.
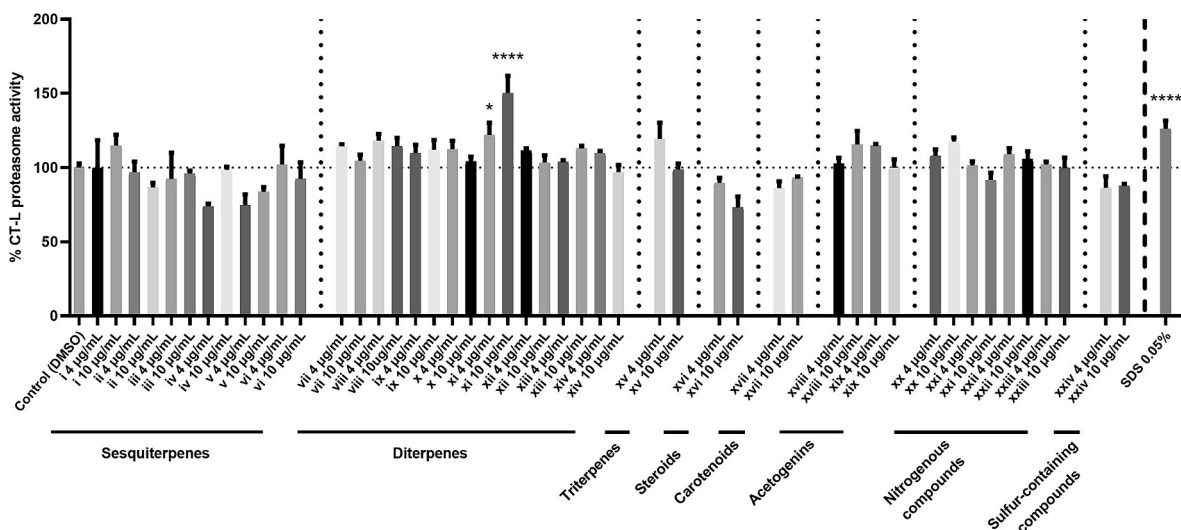
Fig. 2. Screening for proteasome activation *in vitro* by marine metabolites belonging to different chemical classes. Percentage (%) of CT-L proteasome activity following incubation of highly purified human 20S proteasome with DMSO (control) or various concentrations (4 and 10 μg/mL) of each marine metabolite. Different chemical classes were assayed including sesquiterpenes (i-vi), diterpenes (vii-xiv), triterpenes (xv), steroids (xvi), carotenoids (xvii), acetogenins (xviii-xix), nitrogenous compounds (xx-xxiii) and sulfur-containing compounds (xxiv). The mean value of activities in DMSO (control) was set to 100%. SDS 0.05% (w/v) was used as a positive control. All values are reported as the mean of two independent experiments ±SEM. Asterisks denote *p < 0.05, ****p < 0.0001.

3.2. DBTO enhances proteasome activities in cellulo

We then sought to investigate whether treatment with DBTO (**1**) may also enhance proteasome activities *in cellulo*. Early passage (young) HFL1 human primary fibroblasts were treated with different concentrations of DBTO or the diluent (DMSO); 0.3 μg/mL (0.99 μM) DBTO for 2 h significantly enhanced all proteasome activities (Fig. 3b), whereas immunoblot analysis of the catalytic β-type subunits (β1, β2 and β5), as well of α6 and α7 regulatory subunits did not reveal any statistically significant differences (Fig. 3c). This further suggests that the observed differences in proteasome activities do not emerge from alterations in the protein expression of proteasome subunits and thus not from differences of the proteasome levels.

3.3. DBTO improves cellular healthspan in human primary fibroblasts

We and other research groups have reported that proteasome activation delays cellular senescence [9,14,18]. Given the proteasome activating properties of DBTO (**1**), we sought to investigate its effects on the progression of senescence in human primary embryonic fibroblasts. Early passage (young) HFL1 cells (CPD 27) were continuously treated throughout their lifespan with 0.3 μg/mL DBTO (that had been shown to induce proteasome activity *in cellulo* and was used in all subsequent experiments). Even though we did not detect any significant differences in the total number of CPD in the presence of this specific concentration of DBTO (Fig. 4a) or in the presence of two additional concentrations (0.5 and 5 μg/mL DBTO; Fig. S2a), interestingly, DBTO-treated cells maintained their young morphology for longer as compared to the control cultures. This suggested a potentially improved healthspan status in the presence of DBTO. We therefore sought to further investigate this observation. Indeed, DBTO-treated cells exhibited a lower ratio of SA-β-gal positive cells over the total number of cells assayed following continuous treatment with DBTO in two different time points (28 and 60 days) as compared to their control cultures (Fig. 4b). More specifically, 4 weeks after continuous treatment with DBTO or DMSO (control), the ratio of SA-β-gal positive cells over the total number of cells assayed in DBTO-treated cells was 0.281 ± 0.009 as opposed to 0.363 ± 0.006 (p = 0.02) in DMSO-treated cells. This difference was further accentuated after 9 weeks of treatment where the ratio of SA-β-gal positive cells over the total number of cells assayed in DBTO-treated cells was 0.733 ± 0.04

as opposed to 0.944 ± 0.013 (p = 0.002) in DMSO-treated cells. *In vitro* scratch assays revealed an enhanced "wound closure" in DBTO-treated cells compared to DMSO-treated cells; the effect was accentuated at day 60 of their cellular lifespan (Fig. 4c). This result coincides with the reduced numbers of SA-β-gal positive cells at the same time point. Finally, in accordance with the progressive increase of the cyclin-dependent kinase inhibitor p21 (CIP1/WAF1) protein expression levels during replicative senescence [38], decreased protein expression levels of p21 were detected after 28 and 60 days of continuous treatment with DBTO compared to control cultures (Fig. 4d), further supporting healthspan maintenance.

3.4. DBTO improves organismal health status without toxicity incidents

The nematode *C. elegans* is an emerging model in biomedical and environmental toxicology that is highly used for toxicity testing [39]. Moreover, it is increasingly used to reveal the effects of compounds/drugs on the organismal health status [40]. Since we detected an improved cellular healthspan, we also performed a phenotypic analysis of wt nematodes treated with DBTO (**1**) or DMSO to investigate any differences in the fitness of a multicellular organism at day 1 of adulthood (Table 1). Significant positive differences in pharyngeal pumping rate (increase), defecation rate (decrease) and duration of post-embryonic development (increased) were observed in DBTO-treated animals. These differences indicate an enhanced health status of the animals treated with DBTO. Similar changes are observed in long-lived animals [40,41]. More specifically, pharyngeal pumping usually diminishes upon exposure to toxicants. In contrast, the pharyngeal pumping rate was found increased in the presence of DBTO. Although we did not monitor the pharyngeal pumping rate throughout the lifespan of the animals, several compounds that positively affect healthspan have been shown to induce this rate already from day 1 of adulthood [42,43]. Therefore, this DBTO-dependent increase in the pumping rate could also predict a better healthspan during the progression of aging but more experimentation is needed. The shorter defecation cycle can be translated as an enhanced detoxification process thus suggesting ameliorated animal fitness [44]. The number of offspring produced per animal and the capacity of the animals to enter the stress-resistant dauer larvae forms have been identified as sensitive markers that respond to various toxicants [45]. These characteristics
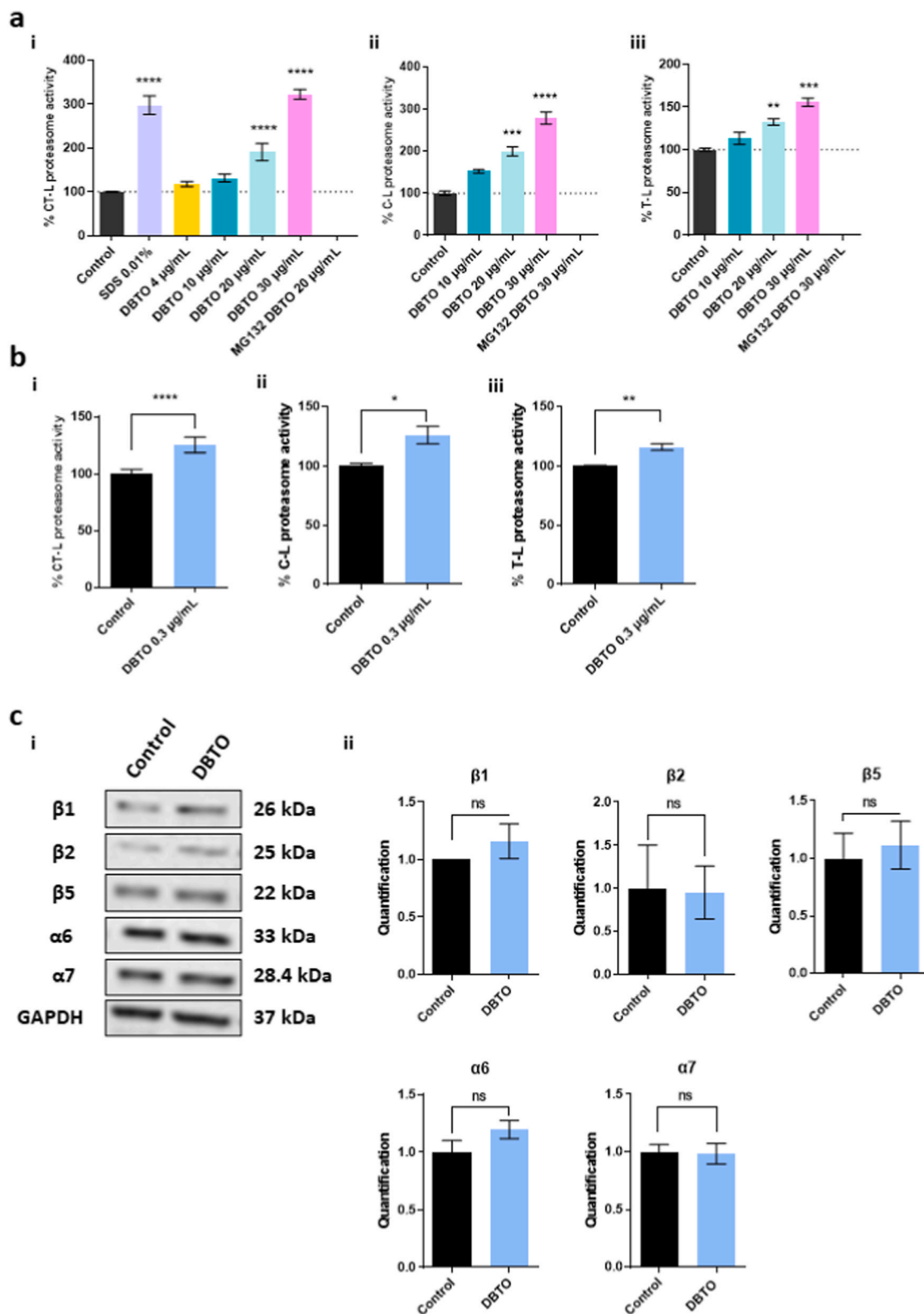
Fig. 3. Proteasome activation *in vitro* and *in cellulo* by DBTO. (a) Percentage (%) of (i) CT-L, (ii) C-L and (iii) T-L proteasome activities following incubation of highly purified human 20S proteasome with DMSO (control) or various concentrations of DBTO. The mean value of activities in DMSO (control) was set to 100%. SDS 0.01% (w/v) was used as a positive control, while 20 μM MG132 was used to ensure assay specificity. Two independent experiments. **(b)** Percentage (%) of (i) CT-L, (ii) C-L and (iii) T-L proteasome activities following 2 h treatment of young HFL1 human primary fibroblasts with the diluent DMSO (control) or 0.3 μg/mL DBTO. The mean value of activities in DMSO-treated cells (control) was set to 100%. Four independent experiments. **(c)** (i) Immunoblot analysis (representative blots) and (ii) quantification of β1, β2, β5, α6 and α7 proteasome subunits in HFL1 human primary fibroblasts treated with 0.3 μg/mL DBTO or the diluent DMSO (control) for 2 h. GAPDH was used as a loading control. Protein levels of DMSO-treated cells (control) were arbitrarily set to 1. Four independent experiments. The molecular weight of each protein appears on the right of each blot. All values are reported as the mean of at least two independent experiments ±SEM. Asterisks denote *p < 0.05, **p < 0.01, ***p < 0.001,****p < 0.0001, ns; not significant.
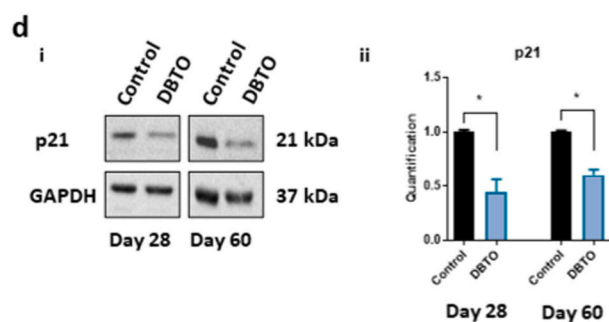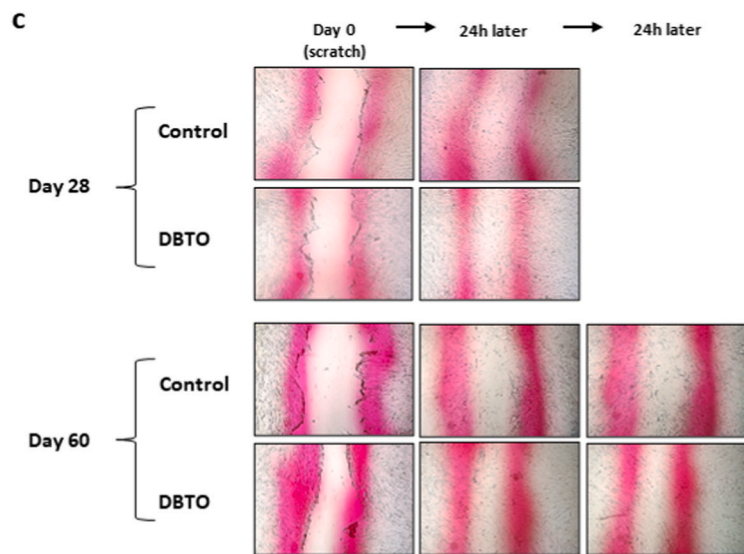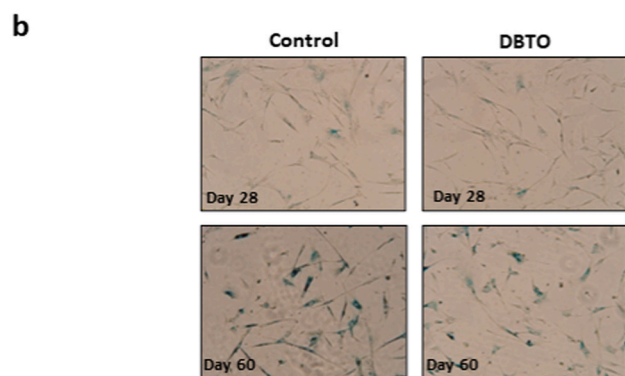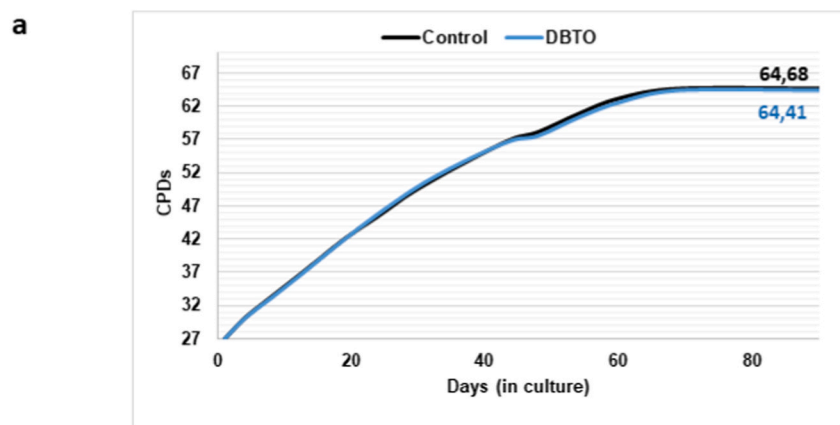
Fig. 4. Treatment with DBTO improves cellular health-span in human primary fibroblasts. (**a**) CPD of HFL1 human primary fibroblasts treated with 0.3 μg/mL DBTO or DMSO throughout their lifespan. Numbers on the graph show the CPD performed by the two cultures at the end of the treatment. A representative graph is shown. (**b**) Representative images of SA-β-gal positive HFL1 cells treated with 0.3 μg/mL DBTO or DMSO throughout their lifespan after 28 and 60 days in culture. (**c**) Representative images of the *in vitro* scratch assay in HFL1 cells treated with 0.3 μg/mL DBTO or DMSO throughout their lifespan at 28 and 60 days in culture. The red lines define the areas of the "technical wound" formed during the scratch assay. Images were taken 24 and 48 h after the scratch formation. The image in the sample at 28 days in culture, 48 h after the scratch formation is not included since both cultures had reached confluency. (**d**) (i) Immunoblot analysis and (ii) quantification of p21 levels in HFL1 cells treated with 0.3 μg/mL DBTO or DMSO throughout their lifespan after 28 and 60 days in culture. GAPDH was used as a loading control. Protein levels of DMSO-treated cells (control) at each time point were arbitrarily set to 1. Two independent experiments. The molecular weight of each protein appears on the right of each blot. All values are reported as the mean of at least two independent experiments ±SEM. Asterisks denote *p < 0.05. (For interpretation of the references to colour in this figure legend, the reader is referred to the Web version of this article.)

Table 1
Phenotypic analysis of wt animals treated with DBTO or DMSO (control).

	Pharyngeal pumping [a], **	Defecation [b], ****	Developmental timing [c], *	Fecundity [d], ns	Dauer formation [e], ns
Control	280.3 ± 2.42	46.54 ± 0.54	54.94 ± 0.31	290.8 ± 6.89	0
DBTO (5 μg/mL)	290.4 ± 2.18	42.12 ± 0.45	56.69 ± 0.29	300.1 ± 4.38	0

* denotes $p < 0.05$, ** denotes $p < 0.01$, **** denotes $p < 0.0001$, ns; not significant.
[a] Pumps in 1 min on day 1 of adulthood.
[b] Duration of defecation cycle in seconds.
[c] Duration of post-embryonic development (hours from egg hatching to L4 stage).
[d] Number of offspring per worm.
[e] Percentage of animals becoming dauer larva at 27 °C.

remained unaltered upon DBTO treatment thus suggesting an intact fitness of the animals and an absence of toxicity for DBTO. Finally, we tested the lifespan extending effects of DBTO in wt *C. elegans* but we did not observe any significant changes in the tested concentrations (0.25, 0.5 and 5 μg/mL), although a tendency was recorded at the concentrations of 0.25 and 0.5 μg/mL (Fig. S2b).

3.5. DBTO confers protection against Aβ-induced toxicity

Proteinopathies, such as AD, are characterized by protein dyshomeostasis which has been directly linked to proteasome dysfunction/inhibition [46]. Moreover, we and others have reported proteasome activation as a potential strategy against aggregation-related diseases [47]. We thus sought to investigate the effects of treatment with DBTO (**1**) on AD progression using two different, well-established *C. elegans* AD models. Initially, we took advantage of the CL4176 strain that expresses the human $Aβ_{1-42}$ peptide in its body wall muscle cells in a temperature-dependent manner. The inducible expression of $Aβ_{1-42}$ leads to a progressive paralytic phenotype due to the gradual formation of Aβ aggregates [48]. CL4176 animals were treated with various concentrations of DBTO (0.5 μg/mL and 10 μg/mL; Fig. S3 μg/mL; Fig. 5); the 5 μg/mL concentration was used throughout the experiments. Treatment of CL4176 animals with 5 μg/mL DBTO resulted in a significant delay of the paralysis onset and progression (Fig. 5a). This positive effect was accompanied by a considerable reduction of total Aβ protein levels by approximately 50% in DBTO-treated animals compared to control animals. A tendency for reduced Aβ oligomeric levels was also observed in CL4176 animals treated with DBTO compared to control animals (Fig. 5b). To further evaluate the Aβ aggregation state *in vivo*, we took advantage of the CL2331 strain that expresses the human $Aβ_{3-42}$ peptide fused to green fluorescent protein (GFP) in its body wall muscle cells. The animals are gradually filled with Aβ aggregates that are visible through confocal microscopy [49]. Treatment of CL2331 animals with DBTO resulted in decreased numbers of Aβ aggregates (Fig. 5c). Overall, our results reveal a DBTO-mediated protection against Aβ-induced toxicity in AD nematode models.

3.6. DBTO enhances the survival of SH-SY5Y cells challenged with exogenously added Aβ peptide in a proteasome activation-dependent manner

To verify the protective effects of DBTO (**1**) against Aβ-induced toxicity in human cells, we took advantage of the human neuroblastoma cell line SH-SY5Y. We firstly verified whether treatment with DBTO induces proteasome activation in these cells. Indeed, SH-SY5Y cells treated with 0.3 μg/mL DBTO for 24 h exhibited significantly enhanced CT-L proteasome activity (Fig. 6a). We have initially verified that survival of SH-SY5Y cells treated with $CM_{Aβ}$ is compromised compared to that of SH-SY5Y cells treated with the respective control (CM). More specifically, SH-SY5Y cells treated with $CM_{Aβ}$ for 24 h were significantly fewer compared to SH-SY5Y cells treated with CM for 24 h (mean cell number CM: $2.36 \times 10^6 \pm 0.071 \times 10^6$, mean cell number $CM_{Aβ}$: $1.77 \times 10^6 \pm 0.047 \times 10^6$, $p < 0.0001$). Consequently, we pre-treated SH-SY5Y

cells with 0.3 μg/mL DBTO or DMSO for 24 h and we then exposed them to $CM_{Aβ}$ or CM in parallel to 0.3 μg/mL DBTO or DMSO. As shown in Fig. 6b, i, treatment of SH-SY5Y cells with CM containing DBTO slightly increased cell numbers. In the case of SH-SY5Y cells challenged with $CM_{Aβ}$, the simultaneous co-treatment with DBTO significantly protected the cells against Aβ-induced toxicity compared to control cultures. The enhanced cell survival was verified through crystal violet staining (Fig. 6b, ii). To verify that the observed improved survival is mainly due to the proteasome activation mediated by DBTO, we repeated the experiment in the presence of 20 nM epoxomicin, a highly specific and irreversible proteasome inhibitor [50]. This epoxomicin concentration is sufficient to block the DBTO-mediated proteasome activation without inducing massive cell death. As shown in Fig. 6c, the protective effect of DBTO in $CM_{Aβ}$-challenged cells was lost in the presence of epoxomicin, thus suggesting that the DBTO-mediated proteasome activation is highly responsible for the recorded enhanced survival against Aβ-mediated proteotoxicity.

3.7. DBTO does not affect other major antioxidant mechanisms

Given the interplay between the proteasome and nuclear factor (erythroid-derived-2)-like 2 (Nrf2) transcription factor [51], we tested whether the observed proteasome activation confers activation of Nrf2 and thus its potential downstream targets; we did not detect any differences in the protein expression levels of its major target genes, namely NQO1 and HO-1. These results along with the lack of changes in the protein expression levels of proteasome subunits (Fig. 3c) suggest an absence of Nrf2 activation in the presence of DBTO (Fig. 7a). We also tested whether treatment with DBTO promotes changes in the redox status of the cells, thus, activating other antioxidant mechanisms that could account for the observed differences. Nevertheless, we did not detect any significant changes of the ROS levels between control and DBTO-treated cells (Fig. 7b). Finally, we tested the activity of SOD as it represents a major antioxidant enzyme; we did not find any significant alterations upon treatment with DBTO (Fig. 7c). Although we cannot rule out the potential activation of additional antioxidant mechanisms that were not examined here, our results suggest that in our conditions the antioxidant mechanism of the proteasome is the one that is mainly activated.

4. Discussion

Accumulating data suggest that proteasome activation may confer positive effects on cellular and organismal healthspan and lifespan. Furthermore, proteasome activation has been recognized as a key strategy against the onset and progression of various proteinopathies, including AD [52]. Consequently, the identification of bioactive compounds with proteasome activating properties has been attracting increasing interest over the recent years. Special attention should be paid to the potential side effects of compounds that activate the proteasome through the regulation of proteasome-related transcription factors, thus, not limiting the activation to the proteasome itself. Therefore, identification of bioactive compounds that may directly
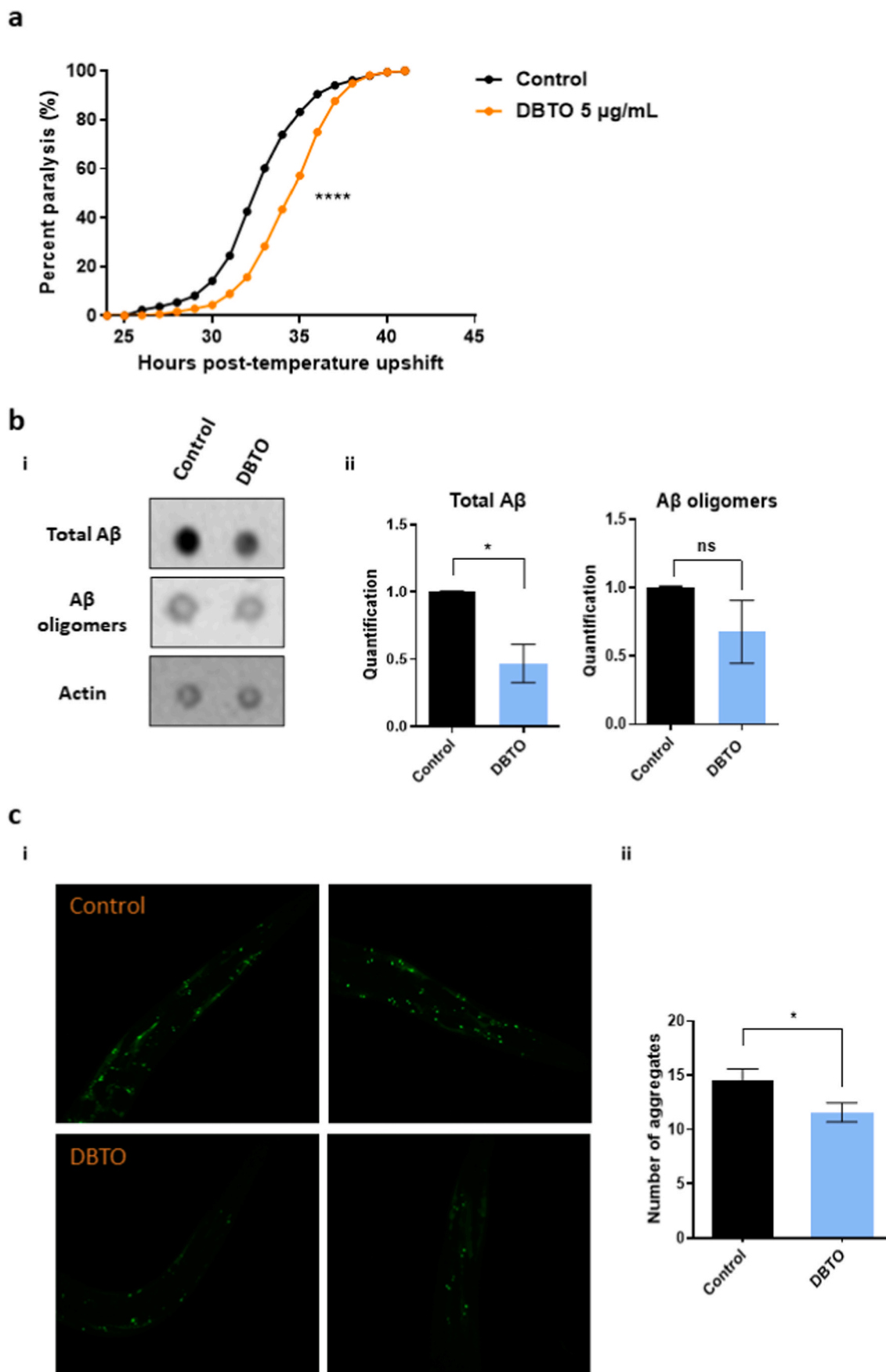
(caption on next page)

Fig. 5. Treatment with DBTO confers decelerated paralysis rate and decreased Aβ deposits in *C. elegans* AD models. (a) Paralysis curve of CL4176 animals expressing human Aβ$_{1-42}$ peptide treated with 5 μg/mL DBTO or DMSO (control). Control: mean = 32.42 ± 0.18, N = 2537/2552; DBTO: mean = 34.45 ± 0.18, N = 2732/2749. N denotes the number of animals that were paralyzed over the total number of animals used (the number of paralyzed animals plus the number of dead and censored animals). Six independent experiments. (b) (i) Dot blot analysis (representative blots) and (ii) quantification of total and oligomeric Aβ levels in CL4176 animals treated with 5 μg/mL DBTO or DMSO (control) and collected when 50% of the control population from (a) was paralyzed. Actin was used as a loading control. Protein levels of DMSO-treated animals (control) were arbitrarily set to 1. Three independent experiments. (c) (i) Representative confocal microscopy images and (ii) number of Aβ aggregates of the anterior area of CL2331 animals expressing the human Aβ$_{3-42}$ peptide conjugated to GFP treated with 5 μg/mL DBTO or DMSO (control) from egg hatching until day 1 of adulthood. Control: mean = 14.56 ± 1.01, N = 27; DBTO: mean = 11.59 ± 0.88, N = 29. N denotes the number of animals observed. Two independent experiments. The values in all experiments are reported as the mean of at least two independent experiments ±SEM. Asterisks denote *p < 0.05, ****p < 0.0001, ns; not significant.
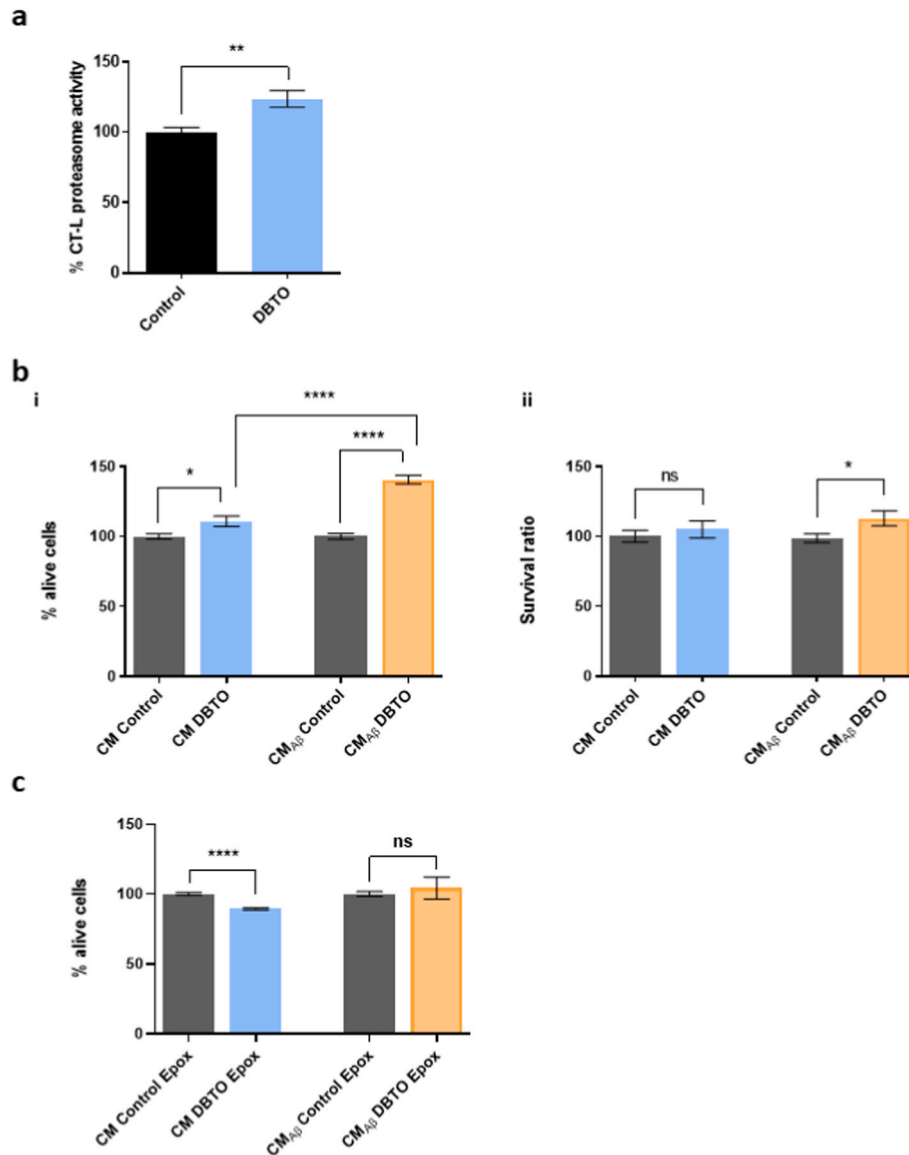

Fig. 6. Treatment with DBTO increases survival of SH-SY5Y neuroblastoma cells challenged with exogenously added Aβ peptide in a proteasome activation-dependent manner. (a) Percentage (%) of CT-L proteasome activity following 24 h treatment of SH-SY5Y neuroblastoma cells with the diluent DMSO (control) or 0.3 μg/mL DBTO. The mean value of activities in DMSO-treated cells (control) was set to 100%. Two independent experiments. (b) (i) Percentage (%) of cell survival and (ii) survival ratio following crystal violet staining of SH-SY5Y neuroblastoma cells treated with DMSO (control) or 0.3 μg/mL DBTO for 24 h and then exposed to CM$_{Aβ}$ or the relative control (CM) and DMSO or 0.3 μg/mL DBTO. The mean value of (i) alive cells and (ii) absorbance in control cultures (CM DMSO and CM$_{Aβ}$ DMSO) was set to 100%. Two independent experiments. (c) Percentage (%) of cell survival of SH-SY5Y neuroblastoma cells treated with DMSO (control) or 0.3 μg/mL DBTO and 20 nM epoxomicin for 24 h and then exposed to CM$_{Aβ}$ or the relative control (CM) and supplemented with DMSO (control) or 0.3 μg/mL DBTO along with 20 nM epoxomicin. The mean value of the number of alive cells in control cultures (CM DMSO Epox and CM$_{Aβ}$ DMSO Epox) was set to 100%. Two independent experiments. All values are reported as the mean of at least two independent experiments ±SEM. Unpaired *t*-test was used for comparison of means. Asterisks denote *p < 0.05, **p < 0.01, **** denotes p < 0.0001. (For interpretation of the references to colour in this figure legend, the reader is referred to the Web version of this article.)

enhance the 20S proteasome activity and function without affecting proteins-nodes, such as transcription factors, is even more valuable. In this study, we have identified for the first time a natural product isolated from the brown alga *D. mediterranea* collected from the island of Karpathos in the Aegean Sea, namely DBTO, which possesses proteasome activating properties. We have shown that DBTO may act as a 20S proteasome activator in cell-free assays but also *in cellulo*. DBTO-dependent proteasome enhancement improves the healthspan of human primary fibroblasts and the health status of wt *C. elegans*, while, most importantly, it confers protection against Aβ-induced proteotoxicity in multiple nematode AD models. Finally, we have shown that

DBTO also confers similar protective effects in human cells of neuronal origin that are exposed to human Aβ peptide in a proteasome activation-dependent manner. Our study identifies for the first time a marine structural proteasome activator and reports its potential healthspan-extending and protective effects against Aβ-induced proteotoxicity in nematode and cellular models.

Compound-mediated proteasome activation may occur through induction of transcription factors that are responsible for the expression of various proteasome subunits or various proteasome regulators, through post-translational modifications of proteasome subunits and regulators or through direct effects on the proteasome conformation [53,54]. The
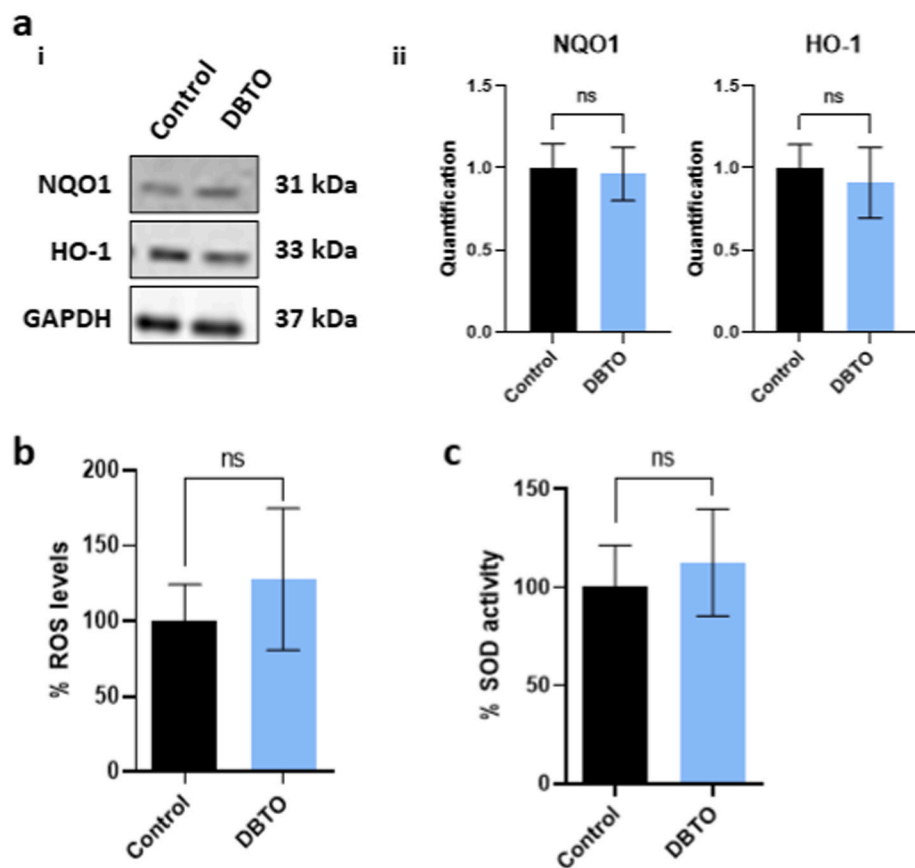
Fig. 7. Lack of DBTO-dependent activation of various antioxidant mechanisms. (**a**) (i) Immunoblot analysis (representative blots) and (ii) quantification of NQO1 and HO-1 Nrf2 target genes in HFL1 human primary fibroblasts treated with 0.3 μg/mL DBTO or the diluent DMSO (control) for 2 h. GAPDH was used as a loading control. Protein levels of DMSO-treated cells (control) were arbitrarily set to 1. Three independent experiments. (**b**) ROS levels and (**c**) percentage (%) of SOD activity in HFL1 human primary fibroblasts treated with 0.3 μg/mL DBTO or the diluent DMSO (control) for 2 h. The mean value of ROS levels and SOD activity in DMSO-treated cells (control) was set to 100%. Three independent experiments. The molecular weight of each protein appears on the right of each blot. All values are reported as the mean of three independent experiments ± SEM. Unpaired *t*-test was used for comparison of means. ns; not significant.

identified compounds that fall into the last category (i.e., structural proteasome activators) are far fewer than those of the remaining categories, especially if we refer to natural compounds. More specifically, fatty acids, such as oleic, linoleic and linolenic acids, have been firstly identified as modulators of the proteasome conformation [55–57]. Likewise, various extracts that are rich in fatty acids, such as extracts from the bee pollen [58], have been suggested to act as proteasome activators. Cellular lipid components, such as lysophosphatidylinositol, ceramides and cardiolipin, have also been shown to modulate proteasome activity [58–60]. Furthermore, we have revealed the proteasome activating properties of oleuropein in the test tube and *in cellulo* [16]. Other natural products with proteasome activating properties include 2-hexyldecanol [61] and betulinic acid [62], among others [1]. Although marine-derived compounds represent a fascinating family of compounds with varied and unique chemical structures that very often possess more potent biological activities, notably, in this list, there are no marine compounds included. In this study, we have identified DBTO (**1**) as the first marine metabolite acting as a structural proteasome activator.

Very few marine compounds and/or extracts have been directly studied for their ability to enhance proteasome activities [26]. Fucoidan, a sulfated polysaccharide from brown algae, is the only marine metabolite that has been shown to enhance CT-L proteasome activity in AD nematode models; nevertheless, the potential proteasome activating properties of fucoidan in cell-free assays was never tested. Moreover, the fucoidan that was active was not chemically characterized in this report [27]. Our preliminary results did not reveal any proteasome activating properties of a particular fucoidan (isolated from *Cystoseira barbata*) assayed but more detailed studies are necessary (unpublished results). The isopropanol extract of the diatom *Phaeodactylum tricornutum* has been shown to promote activation of all three proteasome activities both in human isolated proteasome, as well as in treated human

keratinocytes. As a result, a protective effect against UVA and UVB radiation of the treated cells was observed [63]. Moreover, the *P. tricornutum* lipid-rich extract was able to reduce the levels of oxidized protein in the human *stratum corneum* in human volunteers [64]. Nevertheless, the exact compound that is responsible for these effects was never identified. To our knowledge, DBTO is the first fully characterized marine compound that activates the proteasome in the test tube and *in cellulo*.

It is increasingly accepted that proteasome activation may act protectively against the progression of various proteinopathies [25,65]. This is not surprising as diminished proteasome activity and reduced protein expression levels of various proteasome subunits have been detected in various *in vitro* and *in vivo* AD models, as well as in the brain samples of AD patients [66,67]. We and others have shown that proteasome activation through the overexpression of β5 proteasome subunit decelerated the progression of the AD-like phenotype in the respective nematode (*pbs-5* subunit; [11], *Drosophila* (*Prosβ5* subunit; [23]) and mouse (PSMB5 subunit; [23]) AD models. Similar results were also obtained in nematode AD models through the administration of the proteasome activator 18α-GA [17]. Nevertheless, in the first two studies, we refer to a genetic manipulation which in any case would be difficult to be applicable in humans. In the case of 18α-GA, this compound was shown to transcriptionally activate the proteasome through the induction of the SKN-1/Nrf2 transcription factor, thus, activation of additional unidentified pathways was not excluded. In fact, some Nrf2 target genes were found induced, whereas others not, catalase activity was found elevated, whereas SOD activity was unaltered. In contrast, our current investigation showed that DBTO activates the proteasome in cell-free assays, thus being nominated as a structural enhancer with minimal side pathways activation expected. Our negative results on SOD activation, cellular redox status or Nrf2 target genes expression advocates for this lack of side pathways activation (at least for the ones

tested).

One could ask how DBTO may confer protection against Aβ-induced proteotoxicity. Our results suggest that enhanced proteasome activity leads to decreased protein levels of Aβ oligomers (although statistical significance was not reached) and total Aβ levels. We believe that upon proteasome enhancement, Aβ species get degraded before they get aggregated. Proteasome activation through genetic means [11] or 18α-GA [17] had elicited similar results. In a more recent work, proteasome augmentation (either through genetic overexpression or through novel proteasome agonists) was also shown to enhance the turnover of APP in flies, cultured cells and mice. More importantly, proteasome activity was negatively correlated with protein levels of APP and soluble Aβ$_{42}$ levels in human hippocampal tissues of AD patients, thus suggesting a biological relevance of the findings in the organismal models [23]. Likewise, combination of 18α-GA (responsible for transcriptional proteasome activation) and omega-3 fatty acids (responsible for structural proteasome activation) resulted in a significant decrease of the total percentage of Aβ$_{42}$ coverage in both parietal cortex and hippocampus of 5xFAD mice, without however altering the number of Aβ plaques [24]. The above mentioned studies reveal the possibility of compound-mediated proteasome activation as a potent anti-AD strategy that eventually could end up to clinical trials. Several other natural compounds have also been shown to confer resistance to Aβ-induced proteotoxicity in a proteasome-dependent manner, including resveratrol [68–70], quercetin [71], morin and isoquercitrin [72], ganoderic acid DM [73] and fucoidan [27], among others. Notably, none of the above-mentioned compounds has been characterized as a structural proteasome activator.

We have also revealed a very interesting effect of DBTO on cellular healthspan. Although we did not detect a lifespan-extending effect of DBTO (at least not in the tested concentrations), we report here a robust improvement of the cellular healthspan in the presence of DBTO. Likewise, we report an ameliorated health status of wt nematodes upon DBTO supplementation. Healthspan amelioration has already been shown following proteasome activation through overexpression of the proteasome β5 subunit in *C. elegans* (*pbs-5;* [11]) and in *Drosophila* (*Prosβ5*; [13]), as well as in human primary fibroblasts [14,74]. Our results show that proteasome activation through DBTO is sufficient to promote healthspan improvement, albeit the absence of modulation of the other antioxidant mechanisms. The importance of healthspan amelioration emerges from studies showing that the healthspan is not necessarily correlated with lifespan [75,76] and although both are desired, the scale tilts in favor of the improved healthspan over a more elongated but full of pathologies lifespan. The absence of lifespan extension is rather unexpected since several previous studies have shown that proteasome activation is accompanied by enhanced longevity [47]. We hypothesize that this could be due to variable levels of proteasome activation exerted by the different compounds. However, we cannot exclude the possibility that the lack of activation of other antioxidant mechanisms in addition to the proteasome activation may also account for this effect.

In total, identification of a natural proteasome enhancer that directly affects the 20S proteasome complex function with various downstream positive effects is of pivotal importance. As a natural compound, it is expected to have fewer side effects as compared to synthetic compounds; indeed, our toxicity testing in *C. elegans* confirmed lack of toxicity for DBTO. If a bioactive compound is found in edible species, this can be even more valuable as supplementation can occur through our regular diet; indeed, several species of the brown algal genus *Dictyota* from which DBTO (**1**) was isolated are edible in several parts of the world [77, 78]. The additional advantage of such a compound lies on the fact that its dietary supplementation may start early in life, thus potentially decelerating or targeting the early and often non-traceable negative effects of aging or diseases at initial stages. Finally, as a compound with direct targeted action on the proteasome complex, it presents higher specificity with limited off-target effects. Future studies should focus on the identification of such bioactive compounds, the documentation of their mode of action, the determination of the exact timely doses for a balanced outcome, along with the use of specific carriers for their targeted release wherever and whenever needed.

5. Conclusions

Our study demonstrates the proteasome activating properties of the marine-derived compound DBTO and its positive effects on cellular healthspan and organismal health status along with its protective effects against Aβ-induced proteotoxicity. Our results highlight this bioactive compound as the first reported structural activator from the marine ecosystem that could be potentially used as a healthspan promoter. With additional experimentation in higher eukaryotes, DBTO could be also used in a prophylactic/preventive strategy against Aβ-induced negative effects.

Declaration of competing interest

The authors declare that they have no known competing financial interests or personal relationships that could have appeared to influence the work reported in this paper.

Data availability

Data used for this research is fully available upon request.

Appendix A. Supplementary data

Supplementary data to this article can be found online at https://doi.org/10.1016/j.redox.2022.102462.

References

[1] N. Chondrogianni, M. Sakellari, M. Lefaki, N. Papaevgeniou, E.S. Gonos, Proteasome activation delays aging in vitro and in vivo, Free Radic. Biol. Med. 71 (2014) 303–320, https://doi.org/10.1016/j.freeradbiomed.2014.03.031.

[2] Y. Hou, X. Dan, M. Babbar, Y. Wei, S.G. Hasselbalch, D.L. Croteau, V.A. Bohr, Ageing as a risk factor for neurodegenerative disease, Nat. Rev. Neurol. 15 (2019) 565–581, https://doi.org/10.1038/s41582-019-0244-7.

[3] C.L. Masters, R. Bateman, K. Blennow, C.C. Rowe, R.A. Sperling, J.L. Cummings, Alzheimer's disease, Nat. Rev. Dis. Prim. 1 (2015), 15056, https://doi.org/10.1038/nrdp.2015.56.

[4] A. Rousseau, A. Bertolotti, Regulation of proteasome assembly and activity in health and disease, Nat. Rev. Mol. Cell Biol. 19 (2018) 697–712, https://doi.org/10.1038/s41580-018-0040-z.

[5] Z.C. Gu, C. Enenkel, Proteasome assembly, Cell. Mol. Life Sci. 71 (2014) 4729–4745, https://doi.org/10.1007/s00018-014-1699-8.

[6] R. Raynes, L.C.D. Pomatto, K.J.A. Davies, Degradation of oxidized proteins by the proteasome: distinguishing between the 20S, 26S, and immunoproteasome

proteolytic pathways, Mol. Aspect. Med. 50 (2016) 41–55, https://doi.org/10.1016/j.mam.2016.05.001.

[7] I. Sahu, S.M. Mali, P. Sulkshane, C. Xu, A. Rozenberg, R. Morag, M.P. Sahoo, S.K. Singh, Z. Ding, Y. Wang, S. Day, Y. Cong, O. Kleifeld, A. Brik, M.H. Glickman, The 20S as a stand-alone proteasome in cells can degrade the ubiquitin tag, Nat. Commun. 12 (2021) 6173, https://doi.org/10.1038/s41467-021-26427-0.

[8] M. Lefaki, N. Papaevgeniou, N. Chondrogianni, Redox regulation of proteasome function, Redox Biol. 13 (2017) 452–458, https://doi.org/10.1016/j.redox.2017.07.005.

[9] N. Chondrogianni, M.A. Vasilopoulou, M. Kapetanou, E.S. Gonos, in: S.I.S.B.T.-E. of B.G. Rattan (Ed.), Proteasome Modulation: A Way to Delay Aging?, Academic Press, Oxford, 2020, pp. 92–104, https://doi.org/10.1016/B978-0-12-801238-3.11461-8.

[10] N. Chondrogianni, I. Petropoulos, C. Franceschi, B. Friguet, E.S. Gonos, Fibroblast cultures from healthy centenarians have an active proteasome, Exp. Gerontol. 35 (2000) 721–728, https://doi.org/10.1016/s0531-5565(00)00137-6.

[11] N. Chondrogianni, K. Georgila, N. Kourtis, N. Tavernarakis, E.S. Gonos, Proteasome activation promotes life span extension and resistance to proteotoxicity in Caenorhabditis elegans, Faseb. J. 29 (2015) 611–622, https://doi.org/10.1096/fj.14-252189, 20S.

[12] N.N. Nguyen, A. Rana, C. Goldman, R. Moore, J. Tai, Y. Hong, J. Shen, D.W. Walker, J.H. Hur, Proteasome β5 subunit overexpression improves proteostasis during aging and extends lifespan in Drosophila melanogaster, Sci. Rep. (2019), https://doi.org/10.1038/s41598-019-39508-4.

[13] E. Munkácsy, E.S. Chocron, L. Quintanilla, C.M. Gendron, S.D. Pletcher, A.M. Pickering, Neuronal-specific proteasome augmentation via Prosβ5 overexpression extends lifespan and reduces age-related cognitive decline, Aging Cell (2019), https://doi.org/10.1111/acel.13005.

[14] N. Chondrogianni, C. Tzavelas, A.J. Pemberton, I.P. Nezis, A.J. Rivett, E.S. Gonos, Overexpression of proteasome beta5 assembled subunit increases the amount of proteasome and confers ameliorated response to oxidative stress and higher survival rates, J. Biol. Chem. 280 (2005) 11840–11850, https://doi.org/10.1074/jbc.M413007200.

[15] D. Vilchez, I. Morantte, Z. Liu, P.M. Douglas, C. Merkwirth, A.P.C. Rodrigues, G. Manning, A. Dillin, RPN-6 determines C. elegans longevity under proteotoxic stress conditions, Nature 489 (2012) 263–268, https://doi.org/10.1038/nature11315.

[16] M. Katsiki, N. Chondrogianni, I. Chinou, A.J. Rivett, E.S. Gonos, The olive constituent oleuropein exhibits proteasome stimulatory properties in vitro and confers life span extension of human embryonic fibroblasts, Rejuvenation Res. 10 (2007) 157–172, https://doi.org/10.1089/rej.2006.0513.

[17] N. Papaevgeniou, M. Sakellari, S. Jha, N. Tavernarakis, C.I. Holmberg, E.S. Gonos, N. Chondrogianni, 18α-Glycyrrhetinic acid proteasome activator decelerates aging and Alzheimer's disease progression in Caenorhabditis elegans and neuronal cultures, Antioxidants Redox Signal. 25 (2016) 855–869, https://doi.org/10.1089/ars.2015.6494.

[18] S. Kapeta, N. Chondrogianni, E.S. Gonos, Nuclear erythroid factor 2-mediated proteasome activation delays senescence in human fibroblasts, J. Biol. Chem. 285 (2010) 8171–8184, https://doi.org/10.1074/jbc.M109.031575.

[19] D.M. Huffman, M.J. Schafer, N.K. LeBrasseur, Energetic interventions for healthspan and resiliency with aging, Exp. Gerontol. 86 (2016) 73–83, https://doi.org/10.1016/j.exger.2016.05.012.

[20] J.N. Keller, K.B. Hanni, W.R. Markesbery, Impaired proteasome function in Alzheimer's disease, J. Neurochem. 75 (2000) 436–439, https://doi.org/10.1046/j.1471-4159.2000.0750436.x.

[21] C.G. Almeida, R.H. Takahashi, G.K. Gouras, Beta-amyloid accumulation impairs multivesicular body sorting by inhibiting the ubiquitin-proteasome system, J. Neurosci. Off. J. Soc. Neurosci. 26 (2006) 4277–4288, https://doi.org/10.1523/JNEUROSCI.5078-05.2006.

[22] D. Necchi, S. Lomoio, E. Scherini, Dysfunction of the ubiquitin-proteasome system in the cerebellum of aging Ts65Dn mice, Exp. Neurol. 232 (2011) 114–118, https://doi.org/10.1016/j.expneurol.2011.08.009.

[23] E.S. Chocron, E. Munkácsy, H.S. Kim, P. Karpowicz, N. Jiang, C.E. Van Skike, N. DeRosa, A.Q. Banh, J.P. Palavicini, P. Wityk, L. Kalinowski, V. Galvan, P.A. Osmulski, E. Jankowska, A.M. Pickering, Genetic and pharmacologic proteasome augmentation ameliorates Alzheimer's-like pathology in mouse and fly APP overexpression models, Sci. Adv. 8 (2022), https://doi.org/10.1126/sciadv.abk2252 eabk2252.

[24] A.N. Mladenovic Djordjevic, M. Kapetanou, N. Loncarevic-Vasiljkovic, S. Todorovic, S. Athanasopoulou, M. Jovic, M. Prvulovic, E. Taoufik, R. Matsas, S. Kanazir, E.S. Gonos, Pharmacological intervention in a transgenic mouse model improves Alzheimer's-associated pathological phenotype: involvement of proteasome activation, Free Radic. Biol. Med. 162 (2021) 88–103, https://doi.org/10.1016/j.freeradbiomed.2020.11.038.

[25] M.A. Vasilopoulou, N. Papaevgeniou, Nikoletta chondrogianni, proteasome fate in aging and proteinopathies, in: N. Chondrogianni, E. Pick, A. Gioran (Eds.), Proteostasis and Proteolysis, first ed., CRC Press, 2021, pp. 151–166, https://doi.org/10.1201/9781003048138.

[26] M.A. Vasilopoulou, E. Ioannou, V. Roussis, N. Chondrogianni, Modulation of the ubiquitin-proteasome system by marine natural products, Redox Biol. 41 (2021), 101897, https://doi.org/10.1016/j.redox.2021.101897.

[27] X. Wang, K. Yi, Y. Zhao, Fucoidan inhibits amyloid-β-induced toxicity in transgenic Caenorhabditis elegans by reducing the accumulation of amyloid-β and decreasing the production of reactive oxygen species, Food Funct. 9 (2018) 552–560, https://doi.org/10.1039/c7fo00662d.

[28] M. del Carmen Ramírez, R.A. Toscano, J. Arnason, S. Omar, C.M. Cerda-García-Rojas, R. Mata, Structure, conformation and absolute configuration of new antifeedant dolabellanes from Trichilia trifolia, Tetrahedron 56 (2000) 5085–5091, https://doi.org/10.1016/S0040-4020(00)00423-3.

[29] M.B. Podlisny, B.L. Ostaszewski, S.L. Squazzo, E.H. Koo, R.E. Rydell, D.B. Teplow, D.J. Selkoe, Aggregation of secreted amyloid beta-protein into sodium dodecyl sulfate-stable oligomers in cell culture, J. Biol. Chem. 270 (1995) 9564–9570, https://doi.org/10.1074/jbc.270.16.9564.

[30] H. Frankowski, S. Alavez, P. Spilman, K.A. Mark, J.D. Nelson, P. Mollahan, R.V Rao, S.F. Chen, G.J. Lithgow, H.M. Ellerby, Dimethyl sulfoxide and dimethyl formamide increase lifespan of C. elegans in liquid, Mech. Ageing Dev. 134 (2013) 69–78, https://doi.org/10.1016/j.mad.2012.10.002.

[31] X. Wang, X. Wang, L. Li, D. Wang, Lifespan extension in Caenorhabditis elegans by DMSO is dependent on sir-2.1 and daf-16, Biochem. Biophys. Res. Commun. 400 (2010) 613–618, https://doi.org/10.1016/j.bbrc.2010.08.113.

[32] G.P. Dimri, X. Lee, G. Basile, M. Acosta, G. Scott, C. Roskelley, E.E. Medrano, M. Linskens, I. Rubelj, O. Pereira-Smith, A biomarker that identifies senescent human cells in culture and in aging skin in vivo, Proc. Natl. Acad. Sci. U.S.A. 92 (1995) 9363–9367, https://doi.org/10.1073/pnas.92.20.9363.

[33] C.-C. Liang, A.Y. Park, J.-L. Guan, In vitro scratch assay: a convenient and inexpensive method for analysis of cell migration in vitro, Nat. Protoc. 2 (2007) 329–333, https://doi.org/10.1038/nprot.2007.30.

[34] 1988. $50 K. Wright, Antibodies a laboratory manual, 0-87969-314-2, in: E. Harlow, D. Lane (Eds.), Biochem. Educ., vol. 17Cold Spring Harbor Laboratory, 1989, p. 726, https://doi.org/10.1016/0307-4412(89)90165-9, 220.

[35] R.A. Coleman, D.J. Trader, Methods to discover and evaluate proteasome small molecule stimulators, Molecules 24 (2019), https://doi.org/10.3390/molecules24122341.

[36] A.F. Kisselev, A.L. Goldberg, Monitoring activity and inhibition of 26S proteasomes with fluorogenic peptide substrates, Methods Enzymol. 398 (2005) 364–378, https://doi.org/10.1016/S0076-6879(05)98030-0.

[37] K. Tanaka, T. Yoshimura, A. Ichihara, Role of substrate in reversible activation of proteasomes (multi-protease complexes) by sodium dodecyl sulfate, J. Biochem. 106 (1989) 495–500, https://doi.org/10.1093/oxfordjournals.jbchem.a122880.

[38] G.H. Stein, L.F. Drullinger, A. Soulard, V. Dulić, Differential roles for cyclin-dependent kinase inhibitors p21 and p16 in the mechanisms of senescence and differentiation in human fibroblasts, Mol. Cell Biol. 19 (1999) 2109–2117, https://doi.org/10.1128/MCB.19.3.2109.

[39] M.C.K. Leung, P.L. Williams, A. Benedetto, C. Au, K.J. Helmcke, M. Aschner, J.N. Meyer, Caenorhabditis elegans: an emerging model in biomedical and environmental toxicology, Toxicol. Sci. 106 (2008) 5–28, https://doi.org/10.1093/toxsci/kfn121.

[40] J.A. Rollins, A.C. Howard, S.K. Dobbins, E.H. Washburn, A.N. Rogers, Assessing health span in Caenorhabditis elegans: lessons from short-lived mutants, J. Gerontol. A. Biol. Sci. Med. Sci. 72 (2017) 473–480, https://doi.org/10.1093/gerona/glw248.

[41] C. Huang, C. Xiong, K. Kornfeld, Measurements of age-related changes of physiological processes that predict lifespan of Caenorhabditis elegans, Proc. Natl. Acad. Sci. U.S.A. 101 (2004) 8084–8089, https://doi.org/10.1073/pnas.0400848101.

[42] R. Li, M. Tao, T. Wu, Z. Zhuo, T. Xu, S. Pan, X. Xu, A promising strategy for investigating the anti-aging effect of natural compounds: a case study of caffeoylquinic acids, Food Funct. 12 (2021) 8583–8593, https://doi.org/10.1039/d1fo01383a.

[43] N. Papaevgeniou, A. Hoehn, J.A. Tur, L.-O. Klotz, T. Grune, N. Chondrogianni, Sugar-derived AGEs accelerate pharyngeal pumping rate and increase the lifespan of Caenorhabditis elegans, Free Radic. Res. 53 (2019) 1056–1067, https://doi.org/10.1080/10715762.2019.1661403.

[44] J.J. Ewbank, O. Zugasti, C. elegans: model host and tool for antimicrobial drug discovery, Dis. Model. Mech. 4 (2011) 300–304, https://doi.org/10.1242/dmm.006684.

[45] P.R. Hunt, The C. elegans model in toxicity testing, J. Appl. Toxicol. 37 (2017) 50–59, https://doi.org/10.1002/jat.3357.

[46] S. Paul, Dysfunction of the ubiquitin-proteasome system in multiple disease conditions: therapeutic approaches, Bioessays 30 (2008) 1172–1184, https://doi.org/10.1002/bies.20852.

[47] N. Papaevgeniou, N. Chondrogianni, UPS activation in the battle against aging and aggregation-related diseases: an extended review, Methods Mol. Biol. 1449 (2016) 1–70, https://doi.org/10.1007/978-1-4939-3756-1_1.

[48] C.D. Link, A. Taft, V. Kapulkin, K. Duke, S. Kim, Q. Fei, D.E. Wood, B.G. Sahagan, Gene expression analysis in a transgenic Caenorhabditis elegans Alzheimer's disease model, Neurobiol. Aging 24 (2003) 397–413, https://doi.org/10.1016/s0197-4580(02)00224-5.

[49] C.D. Link, V. Fonte, C.M. Roberts, B. Hiester, M.A. Silverman, G.H. Stein, The beta amyloid peptide can act as a modular aggregation domain, Neurobiol. Dis. 32 (2008) 420–425, https://doi.org/10.1016/j.nbd.2008.08.003.

[50] N. Sin, K.B. Kim, M. Elofsson, L. Meng, H. Auth, B.H. Kwok, C.M. Crews, Total synthesis of the potent proteasome inhibitor epoxomicin: a useful tool for understanding proteasome biology, Bioorg. Med. Chem. Lett. 9 (1999) 2283–2288, https://doi.org/10.1016/s0960-894x(99)00376-5.

[51] M.-K. Kwak, N. Wakabayashi, J.L. Greenlaw, M. Yamamoto, T.W. Kensler, Antioxidants enhance mammalian proteasome expression through the Keap1-Nrf2 signaling pathway, Mol. Cell Biol. 23 (2003) 8786–8794, https://doi.org/10.1128/MCB.23.23.8786-8794.2003.

[52] N. Chondrogianni, K. Voutetakis, M. Kapetanou, V. Delitsikou, N. Papaevgeniou, M. Sakellari, M. Lefaki, K. Filippopoulou, E.S. Gonos, Proteasome activation: an

innovative promising approach for delaying aging and retarding age-related diseases, Ageing Res. Rev. 23 (2015) 37–55, https://doi.org/10.1016/J.ARR.2014.12.003.

[53] E. Panagiotidou, N. Chondrogianni, We are what we eat: ubiquitin-proteasome system (UPS) modulation through dietary products, Adv. Exp. Med. Biol. 1233 (2020) 329–348, https://doi.org/10.1007/978-3-030-38266-7_15.

[54] M. Kapetanou, S. Athanasopoulou, E.S. Gonos, Transcriptional regulation of proteostatic mechanisms, in: N. Chondrogianni, E. Pick, A. Gioran (Eds.), Proteostasis and Proteolysis, first ed., 2021, pp. 31–44, https://doi.org/10.1201/9781003048138.

[55] B. Dahlmann, M. Rutschmann, L. Kuehn, H. Reinauer, Activation of the multicatalytic proteinase from rat skeletal muscle by fatty acids or sodium dodecyl sulphate, Biochem. J. 228 (1985) 171–177, https://doi.org/10.1042/bj2280171.

[56] N. Watanabe, S. Yamada, Activation of 20S proteasomes from spinach leaves by fatty acids, Plant Cell Physiol. 37 (1996) 147–151, https://doi.org/10.1093/oxfordjournals.pcp.a028925.

[57] A.F. Kisselev, D. Kaganovich, A.L. Goldberg, Binding of hydrophobic peptides to several non-catalytic sites promotes peptide hydrolysis by all active sites of 20 S proteasomes. Evidence for peptide-induced channel opening in the alpha-rings, J. Biol. Chem. 277 (2002) 22260–22270, https://doi.org/10.1074/jbc.M112360200.

[58] I. Ohkubo, S. Gasa, C. Namikawa, A. Makita, M. Sasaki, Human erythrocyte multicalatytic proteinase: activation and binding to sulfated galacto- and lactosylceramides, Biochem. Biophys. Res. Commun. 174 (1991) 1133–1140, https://doi.org/10.1016/0006-291x(91)91538-n.

[59] K. Matsumura, K. Aketa, Proteasome (multicatalytic proteinase) of sea urchin sperm and its possible participation in the acrosome reaction, Mol. Reprod. Dev. 29 (1991) 189–199, https://doi.org/10.1002/mrd.1080290215.

[60] I. Ruiz de Mena, E. Mahillo, J. Arribas, J.G. Castaño, Kinetic mechanism of activation by cardiolipin (diphosphatidylglycerol) of the rat liver multicatalytic proteinase, Biochem. J. 296 (Pt 1) (1993) 93–97, https://doi.org/10.1042/bj2960093.

[61] T. Hakozaki, T. Laughlin, S. Zhao, J. Wang, D. Deng, E. Jewell-Motz, L. Elstun, A regulator of ubiquitin-proteasome activity, 2-hexyldecanol, suppresses melanin synthesis and the appearance of facial hyperpigmented spots, Br. J. Dermatol. 169 (Suppl) (2013) 39–44, https://doi.org/10.1111/bjd.12364.

[62] L. Huang, P. Ho, C.-H. Chen, Activation and inhibition of the proteasome by betulinic acid and its derivatives, FEBS Lett. 581 (2007) 4955–4959, https://doi.org/10.1016/j.febslet.2007.09.031.

[63] A.-L. Bulteau, M. Moreau, A. Saunois, C. Nizard, B. Friguet, Algae extract-mediated stimulation and protection of proteasome activity within human keratinocytes exposed to UVA and UVB irradiation, Antioxidants Redox Signal. 8 (2006) 136–143, https://doi.org/10.1089/ars.2006.8.136.

[64] C. Nizard, S. Poggioli, C. Heusèle, A.-L. Bulteau, M. Moreau, A. Saunois, S. Schnebert, C. Mahé, B. Friguet, Algae extract protection effect on oxidized protein level in human stratum corneum, Ann. N. Y. Acad. Sci. 1019 (2004) 219–222, https://doi.org/10.1196/annals.1297.036.

[65] D.E. George, J.J. Tepe, Advances in proteasome enhancement by small molecules, Biomolecules 11 (2021), https://doi.org/10.3390/biom11121789.

[66] I. Fernández-Cruz, E. Reynaud, Proteasome subunits involved in neurodegenerative diseases, Arch. Med. Res. 52 (2021) 1–14, https://doi.org/10.1016/j.arcmed.2020.09.007.

[67] S. Oddo, The ubiquitin-proteasome system in Alzheimer's disease, J. Cell Mol. Med. 12 (2008) 363–373, https://doi.org/10.1111/j.1582-4934.2008.00276.x.

[68] P. Marambaud, H. Zhao, P. Davies, Resveratrol promotes clearance of Alzheimer's disease amyloid-beta peptides, J. Biol. Chem. 280 (2005) 37377–37382, https://doi.org/10.1074/jbc.M508246200.

[69] C. Regitz, E. Fitzenberger, F.L. Mahn, L.M. Dußling, U. Wenzel, Resveratrol reduces amyloid-beta (Aβ₁-₄₂)-induced paralysis through targeting proteostasis in an Alzheimer model of Caenorhabditis elegans, Eur. J. Nutr. 55 (2016) 741–747, https://doi.org/10.1007/s00394-015-0894-1.

[70] R. Corpas, C. Griñán-Ferré, E. Rodríguez-Farré, M. Pallàs, C. Sanfeliu, Resveratrol induces brain resilience against alzheimer neurodegeneration through proteostasis enhancement, Mol. Neurobiol. 56 (2019) 1502–1516, https://doi.org/10.1007/s12035-018-1157-y.

[71] C. Regitz, L.M. Dußling, U. Wenzel, Amyloid-beta (Aβ₁-₄₂)-induced paralysis in Caenorhabditis elegans is inhibited by the polyphenol quercetin through activation of protein degradation pathways, Mol. Nutr. Food Res. 58 (2014) 1931–1940, https://doi.org/10.1002/mnfr.201400014.

[72] V. Carmona, S. Martín-Aragón, J. Goldberg, D. Schubert, P. Bermejo-Bescós, Several targets involved in Alzheimer's disease amyloidogenesis are affected by morin and isoquercitrin, Nutr. Neurosci. 23 (2020) 575–590, https://doi.org/10.1080/1028415X.2018.1534793.

[73] S. Chakrabortee, Y. Liu, L. Zhang, H.R. Matthews, H. Zhang, N. Pan, C. Cheng, S. Guan, D. Guo, Z. Huang, Y. Zheng, A. Tunnacliffe, Macromolecular and small-molecule modulation of intracellular Aβ42 aggregation and associated toxicity, Biochem. J. 442 (2012) 507–515, https://doi.org/10.1042/BJ20111661.

[74] N. Chondrogianni, F.L.L. Stratford, I.P. Trougakos, B. Friguet, A.J. Rivett, E.S. Gonos, Central role of the proteasome in senescence and survival of human fibroblasts: induction of a senescence-like phenotype upon its inhibition and resistance to stress upon its activation, J. Biol. Chem. 278 (2003) 28026–28037, https://doi.org/10.1074/jbc.M301048200.

[75] A. Bansal, L.J. Zhu, K. Yen, H.A. Tissenbaum, Uncoupling lifespan and healthspan in Caenorhabditis elegans longevity mutants, Proc. Natl. Acad. Sci. U.S.A. 112 (2015) E277–E286, https://doi.org/10.1073/pnas.1412192112.

[76] K.E. Fischer, J.M. Hoffman, L.B. Sloane, J.A.L. Gelfond, V.Y. Soto, A.G. Richardson, S.N. Austad, A cross-sectional study of male and female C57BL/6Nia mice suggests lifespan and healthspan are not necessarily correlated, Aging (Albany NY) 8 (2016) 2370–2391, https://doi.org/10.18632/aging.101059.

[77] O. De Clerck, E. Coppejans, W.P. Van Reine, Dictyota 2001 (2001), 139260. http://lib.ugent.be/catalog/pug01.

[78] L. Pereira, Edible Seaweeds of the World, first ed., CRC Press, 2016 https://doi.org/10.1201/b19970.